Spring 4-4-2019

TEMPERATURE OPTIMIZATION OF LACTIC ACID BATCH FERMENTATION BY LACTOBACILLUS PENTOSUS AND ITS KINETIC MODEL

Jiaqi Huang
jhuang42@syr.edu

TEMPERATURE OPTIMIZATION OF LACTIC ACID BATCH FERMENTATION BY *LACTOBACILLUS PENTOSUS* AND ITS KINETIC MODEL

by

Jiaqi Huang

A thesis
submitted in partial fulfillment
of the requirements for the
Master of Science Degree
State University of New York
College of Environmental Science and Forestry
Syracuse, New York
April 2019

Department of Paper and Bioprocess Engineering

Approved by:
Shijie Liu, Major Professor
Martin Dovciak, Chair, Examining Committee
Bandaru V. Ramarao, Department Chair
S. Scott Shannon, Dean, The Graduate School

Acknowledgements

I would first like to thank my major Advisor, Prof. Shijie Liu. You supported me greatly and were always willing to help me, giving me advice on research, jobs and goals for my future. Furthermore, I would like to thank my committee members, Dr. Klaus Dölle, Prof. Thomas E Amidon, for their valuable comments and suggestions. You definitely provided me with the tools that I needed to choose the right direction and successfully complete my dissertation.

I would especially like to thank Mr. Dave Kiemle for his support with NMR analytical work. I would also like to acknowledge my research group members: Xiaolin Qu, Wei Dai, Hanchi Chen, Xiaoyan Chen, Guoyu Dong, Lingkun Li, Yue Liu and Botao Zhao for their valuable input and help.

My greatest gratitude goes to my parents, Mr. and Mrs. Huang along with my best friends, Qianhui Zhou and Chengyan Jing. Special thanks to my boyfriend, Jianfei Wang. You are always there for me, giving me the strength of mind to keep moving forward. I am grateful for all your love, support, help, and understanding.

Table of Contents

LIST OF ABBREVIATIONS AND SYMBOLS

Abbreviations

ADP	Adenosine diphosphate
AHA	Alpha Hydroxy Acid
ATCC	American Type Culture Collection
ATP	Adenosine triphosphate
EMP	Embden-Meyerhof Parnas
E. coli	*Escherichia coli*
GC	Gas chromatography
GRAS	Generally recognized as safe
HPLC	High performance liquid chromatography
HSQC	Heteronuclear single quantum correlation
LA	Lactic acid
LAB	Lactic acid bacteria
L. pentosus	*Lactobacillus pentosus*
NMR	Nuclear magnetic resonance
OD	Optical density
PK	Phosploketolase
PLA	Polylactic acid
SUNY- ESF	State University of New York College of Environmental Science and Forestry

TSP	Trimethylsilyl propionate

Symbols

N	the nitrogen source concentration, g/L
k_d	the specific death rate, h^{-1}
K	the saturation constant, g/L
P	the product concentration, g/L
r	the reaction rate, g/(L•h)
γF	the yield factor, g/g
S	the limiting substrate concentration, g/L
t	the fermentation time, h
μ	the specific rate, h^{-1}
V	the reactor volume, L
X	the cell biomass concentration, g/L

LIST OF TABLES

LIST OF FIGURES

LIST OF APPENDICES

Abstract

J. Huang. Increased Lactic Acid Batch Fermentation Process by *Lactobacillus pentosus* Its Kinetic Model, 77 pages, 3 tables, 27 figures, 2019. APA style guide used.

Currently, lactic acid (LA) is being widely utilized in food industry, chemical industry and poly (lactic acid) synthesis. However, the search for the most favorable fermentation conditions is still desired for the successful commercial development of cost competitive processes. In this work, the effects of temperature on LA batch fermentation from glucose by *Lactobacillus pentosus* (*L. pentosus*) were studied. In batch fermentation of pH 6.0, the optimal temperature is 35 ℃ (agitation speed at 150 rpm, and air flow rate at 25 mL/min), and lower temperature leads to better cell growth while higher temperature results in more efficient glucose utilization and more productive LA generation. A kinetic model was developed to properly simulate batch LA production at 35 ℃ and pH 6.0 from glucose by *L. pentosus*.

Key words: lactic acid, fermentation, temperature, kinetic modeling

Jiaqi Huang
Candidate for the degree of Master of Science, May 2019
Shijie Liu, Ph.D.
Department of Paper and Bioprocess engineering
State University of New York College of Environmental Science and Forestry,
Syracuse, New York

CHAPTER 1: INTRODUCTION

1.1 Introduction

Traditionally, LA and its derivatives are applied in the food industry, chemical industry, cosmetics and pharmaceutical industry (Vijayakumar, Aravindan & Viruthagiri, 2008). However, LA has become a valuable chemical, as a monomer used in the production of polylactic acid (PLA). Its production is significantly increasing to supply the feedstock for PLA production (Alsaheb et al., 2015).

In industry, LA is produced by bacterial fermentation or by chemical synthesis from acetaldehyde (Li & Cui, 2010). Approximately 90% of the total LA production is obtained from microbial fermentation. However, many parameters influence the efficiency of a fermentation process (Hofvendahl & Hahn-Hägerdal, 2000). Therefore, there is a search for the most favorable fermentation conditions, which vary depending on the microorganism, to use in promoting the development of economically competitive processes. In addition, the study of the kinetics for cell growth, product formation and substrate utilization would be helpful for fermentation process development, optimization and bioreactor design (Akpa, 2012).

This dissertation presents the investigation of temperature effects and a kinetics study of LA production via the batch fermentation process.

1.2 Objectives of study

The objectives of this study are:

1. To study the kinetics of glucose utilization and LA production by *L. pentosus* in a batch fermentation process.

2. To study the effects of temperature on the cell growth of *L. pentosus*, glucose utilization and LA production.

3. To develop a kinetic model to simulate the cell growth of *L. pentosus*, glucose utilization and LA production.

1.3 Dissertation Outline

In Chapter 2, a literature review related to LA production and the *L. pentosus* metabolic pathway and parameters effecting fermentation is presented.

In Chapter 3, the experimental methods employed in this study are explained. Seed culture preparation and fermentation procedures are described, and the techniques for determination of biomass, glucose and LA concentration are detailed.

In Chapter 4, batch production of LA from glucose by *L. pentosus* is examined with focus on the effects of temperature on the cell growth of *L. pentosus*, glucose utilization and LA production. A kinetic study of batch production of LA from glucose by *L. pentosus* is also conducted, providing a mathematical model of *L. pentosus* cell growth rate, product formation rate and glucose utilization rate via batch fermentation process.

In Chapter 5, the findings of this study are presented, along with the recommendations for future studies.

CHAPTER 2: LITERATURE REVIEW

This chapter presents a brief review of LA production.

2.1 Introduction

LA, or 2-hydroxypropanoic acid, is a hygroscopic non-toxic organic compound with the formula $CH_3CH(OH)COOH$, also named milk acid. It is white and water-soluble in its solid state and colorless in its liquid state. LA is chiral, consisting of two optical isomers with one known as L-(+)-LA or (S)-LA and the other, its mirror image, as D-(−)-LA or (R)-LA (Martinez et al., 2013). DL-LA or racemic LA, a mixture of the two in equal amounts, is miscible with water and with ethanol above its melting point which is around 17 or 18 °C. Due to the presence of a hydroxyl group and a carboxyl group, LA can be self-esterified, dimerized to form a ring, or polymerized to form a polymer. (Vu et al., 2013).

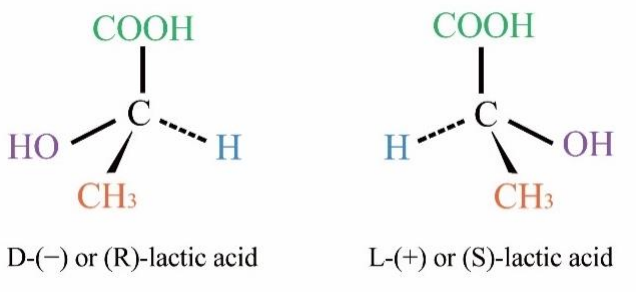

Figure 2.1 Structure of D (−) and L (+) isomers of LA (redrawn based on Martinez et al., 2013).

2.2 LA application

As an industrially important product, LA and its derivatives have a wide range of applications in the food industry, chemical industry, cosmetics and pharmaceutical

industry. Furthermore, LA can polymerize to obtain polylactic acid which can be further used as a biodegradable polymeric material (Dusselier, Van Wouwe, Dewaele, Makshina, & Sels, 2013).

2.2.1 Food applications

LA is found primarily in sour milk products, such as koumiss, yogurt, kefir, and some cottage cheeses. It is approved for the use as a food ingredient by regulatory agencies in the EU, USA, Australia and New Zealand. LA can be used in a variety of processed foods like candy, beverages, bakery products, canned fruit and vegetables, jams and jellies, as an acidulant, color maintaining and pH buffering agent (Leroy & De Vuyst, 2004). In beermaking, a bacterial process, adding the proper amount of LA can adjust the pH value to promote saccharification, facilitate yeast fermentation, improve beer quality and extend the shelf life. Because of its preservative effect, it can also be used as a decontaminant during meat processing. In terms of seasoning, the addition of a certain amount of LA can stabilize and inhibit the growth of microorganisms in the product as well as improving the taste (De Vuyst & Leroy, 2007).

2.2.2 Pharmaceutical and cosmetic applications

LA can be directly formulated into medicines or daily health care products, working as a preservative, carrier, cosolvent, pH adjuster, etc. in medicine. LA vapor can effectively kill bacteria in the air in wards and operating rooms. As the most effective type of Alpha Hydroxy Acid (AHA) and with little irritation, LA is widely used in various skin care products to adjust acidity and for its disinfectant and

keratolytic properties (Datta & Henry, 2006). LA can also be used as a moisturizer in many toiletries, such as shampoos, soaps and body lotion, and as a pH regulator in soaps, reducing the loss of moisture during storage and thus preventing the soap from cracking (Narayanan, Roychoudhury, & Srivastava, 2004).

2.2.3 Chemical applications

In the textile and tanning industry, LA can be used to pretreat raw materials, which makes them softer, easier to dye and more lustrous. In the cigarette industry, LA can be applied to maintain tobacco moisture, neutralize nicotine and reducing other harmful substances to improve tobacco quality (Narayanan et al., 2004). Due to its unique complexation constant for nickel, LA is often used in the nickel plating process and as a buffer and stabilizer in the plating bath at the same time. In the microelectronics industry, its unique high purity and low metal content meets the high requirements for semiconductor quality (Datta & Henry, 2006). In addition, LA is used as a pH regulator and a synthetic agent in a variety of water-based coating systems. LA works better for washing and cleaning compared to other traditional organic detergents with the functions of a cleansing and anti-microbial agent, so it can be applied to many descaling products (Wee, Kim, & Ryu, 2006).

2.2.4 Biomaterial

As a leading example of bio-based plastics, PLA presents a potential to reduce the dependence on fossil fuels and the related environmental impacts (Thongchul, 2013). PLA can be drawn into a silk-spun line, a good surgical suture. After the cut is healed,

there is no need to remove the thread, as the body can degrade it into LA and it then to be absorbed by the human body without adverse consequences. This eliminates the need for suturing the second operation for the removal of the surgical suture in the body. The polymer compound can also be used as a binder in organ transplantation and bone grafting (Lunt, 1998). The special characteristics of PLA, such as GRAS (generally regarded as safe) status, biodegradability, comparable cost and effective antimicrobial activity, make it a promising material in antimicrobial food packaging (Jin & Zhang, 2008). In addition, PLA is used in the production of agricultural film, taking the place of hydrocarbon based plastic film. After use, It can be decomposed by bacteria and then incorporated into the soil. (Agarwal, Koelling, & Chalmers, 1998).

2.3 Fermentative production

LA can be produced both naturally and synthetically. In industry, LA is produced by bacterial fermentation, where lactic acid bacteria (LAB) convert simple carbohydrates such as glucose, sucrose, or galactose to LA, or by chemical synthesis from acetaldehyde, which is available from coal or crude oil (Wee et al., 2006). Fermentative production can obtain an optically pure product by choosing a strain of LAB producing only one of the isomers, whereas synthetic production always results in a racemic mixture of LA. Moreover, renewable resources, such as starch and cellulose, can be fed as substrates in fermentative production (Wang, Tashiro, & Sonomoto, 2015), which does not give any net contribution to carbon dioxide emissions or use limited oil- and fossil-fuel-based sources.

2.3.1 Batch reactor

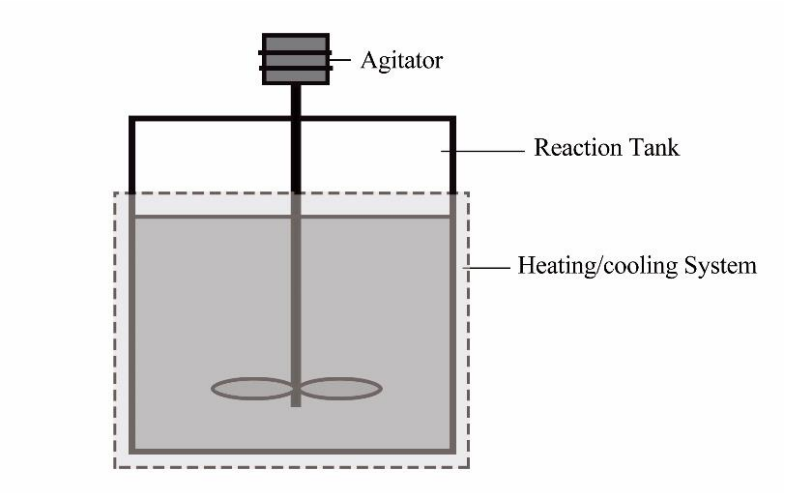

Figure 2.2 Schematic diagram of a batch reactor.

A batch reactor is the simplest type of reaction vessels, typically consisted of a tank with an agitator and integral heating/cooling system (Bieler, 2004). Prior to setting the reaction conditions, all reactants and solvents are added to the batch reactor and no reactant is put in nor product is taken out until the reaction is complete. Both heat generation and concentrations in the batch reactor vary during the reaction process (Foutch & Johannes, 2017). Batch reactors are often used in pharmaceutical production, industrial processes like waste water treatment, or laboratories, such as small-scale production, inducing fermentation processes and experiments of reaction kinetics, volatiles and thermodynamics (Krishna, 2013). Batch reactors are not always referred to as reactors but a name reflecting the role they perform, crystallizer, bioreactor or fermenter (Towler & Sinnott, 2012). Batch reactors have the advantage of obtaining high conversions by leaving the reactants in for long periods of time. However, they are also generally considered expensive to run, difficult to scale up, as well as having potential variability of products from batch to batch (Fogler, 2010).

2.3.2 Nutrient required for *L. pentosus* growth

L. pentosus, the microorganism applied in this study, is one of the LAB strains, which are rod shaped bacteria. It has LA as the major end product from energy-conserving fermentation of sugars. *L. pentosus* is one of the few LAB organism which has been demonstrated to metabolize hexoses to produce almost exclusively LA or metabolize pentoses to produce LA with acetic as the main byproduct. (Garde, Jonsson, Schmidt, & Ahring, 2002). LAB is a general term for bacteria that are capable of producing LA from fermentable carbohydrates, consisted of the Gram-positive genera: *Carnobacterium, Enterococcus, Lactobacillus, Lactococcus, Leuconostoc, Oenococcus, Pediococcus, Streptococcus, Tetragenococcus, Vagococcus, and Weissella*. Most LAB are considered GRAS with high acid tolerance at pH 5 and lower and the optimal temperature for growth, which varies between the genera, from 20 to 45°C (Axelsson & Ahrné, 2000).

Like many heterotrophic microorganisms, *L. pentosus* has limited ability to decompose carbohydrates and synthesize organic compounds, due to its relatively simple enzyme system. Therefore, *L. pentosus* requires supplement nutrients like amino acids, vitamins and minerals as well as fermentable carbohydrates and nitrogen sources for optimal growth (Todorov & Dicks, 2004). The carbon source used is usually from monosaccharides like glucose or oligosaccharides, providing energy in cells and metabolites. Hydrolysis products of protein, such as the peptide, amino acids and peptone, can be fed as sources of nitrogen. Some of the needed minerals can be obtained from nutrients, and the others are provided as inorganic salts, with manganese being

the most influential.

Table 2.1 Nutrients of the fermentation broth in this study.

Component	Element	Physiological Function
Glucose	Carbon	Constituent of organic cellular material, the energy source
Yeast Extract	Nitrogen	Constituent of proteins, nucleic acids and coenzymes
K2HPO4 & K2HPO4	Phosphorus	Constituent of nucleic acids, phospholipids, nucleotides and certain coenzymes
	Potassium	Principal inorganic cation in cells and cofactor for some enzymes

2.3.3 Metabolic pathway in fermentation by *L. pentosus*

LAB ferment sugars via different pathways resulting in homo-, hetero-, or mixed acid fermentation (Fig 2.3). In homofermentation, the Embden–Meyerhof–Parnas (EMP) pathway is used, producing only LA as the end product of glucose metabolism (Bustos, Moldes, Cruz, & Domínguez, 2005). According to the overall stoichiometry below:

$$\text{Glucose} + 2\ \text{ADP} + 2\ \text{Pi} \rightarrow 2\ \text{Lactic Acid} + 2\ \text{ATP},$$

homofermentation should theoretically yield 2 moles of LA per mole of consumed glucose with a theoretical yield ($Y_{P/S}$) of 1 g/g (g of product per g of substrate). But the experimental yields are usually lower (0.74 - 0.99 g/g), because a portion of the carbon source is used for cell growth. In heterofermentation, the phosphoketolase (PK) pathway is applied, forming equimolar amounts of LA, carbon dioxide and ethanol, following the overall reaction:

$$\text{Glucose} + 2\ \text{ADP} + 2\ \text{Pi} \rightarrow \text{Lactic acid} + CO_2 + \text{Ethanol} + 2\ \text{ATP}.$$

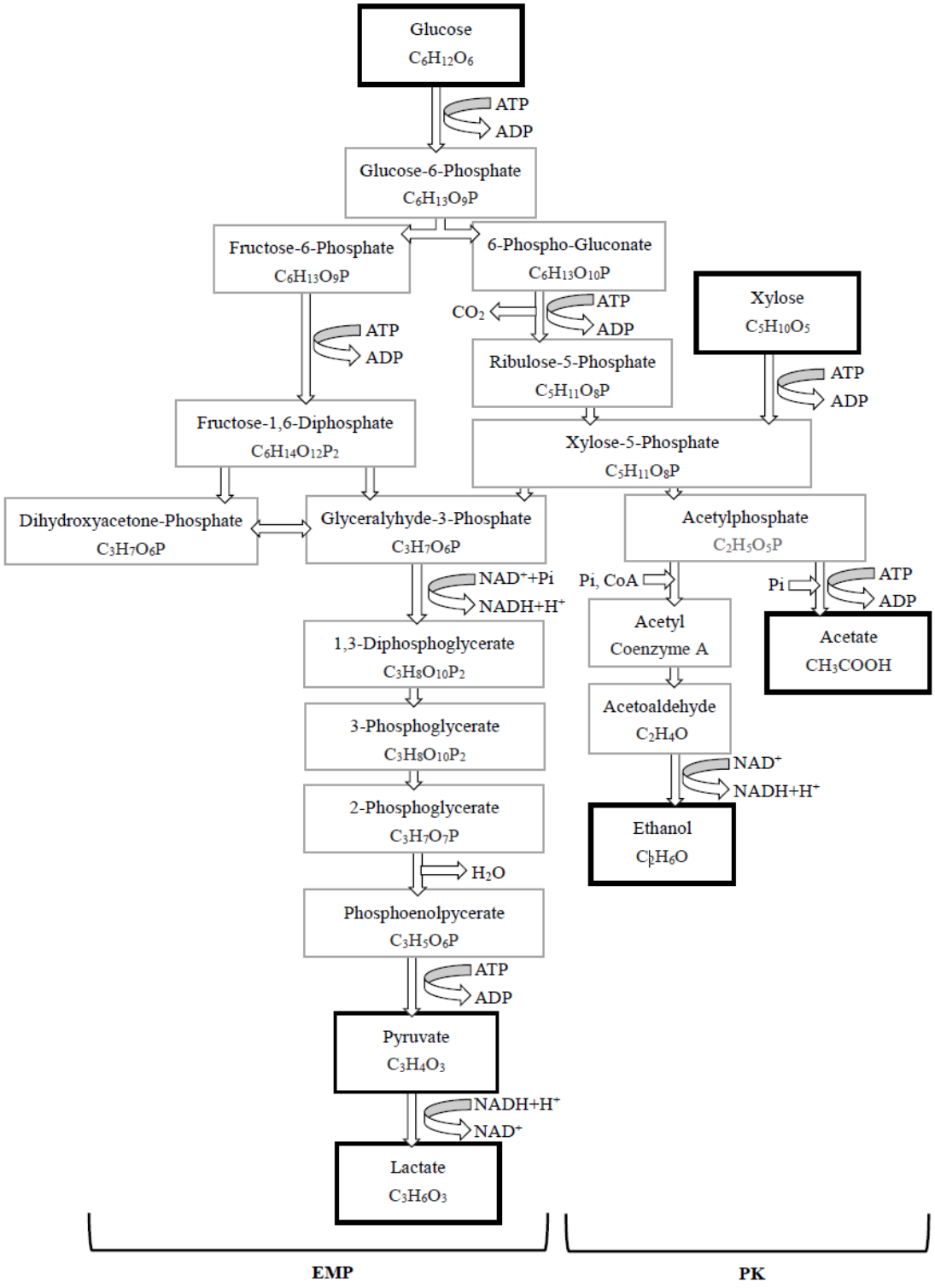

Figure 2.3 Illustration of EMP pathway and PK pathway in the left and right sides, respectively (redrawn based on Martinez et al., 2013).

2.3.4 Parameters affecting fermentation

The main factors affecting the efficiency of a fermentation process can be

summarized as microorganism, carbon source, nitrogen source, fermentation mode, pH and temperature, immobilization and recirculation of cells (Hofvendahl & Hahn–Hägerdal, 2000).

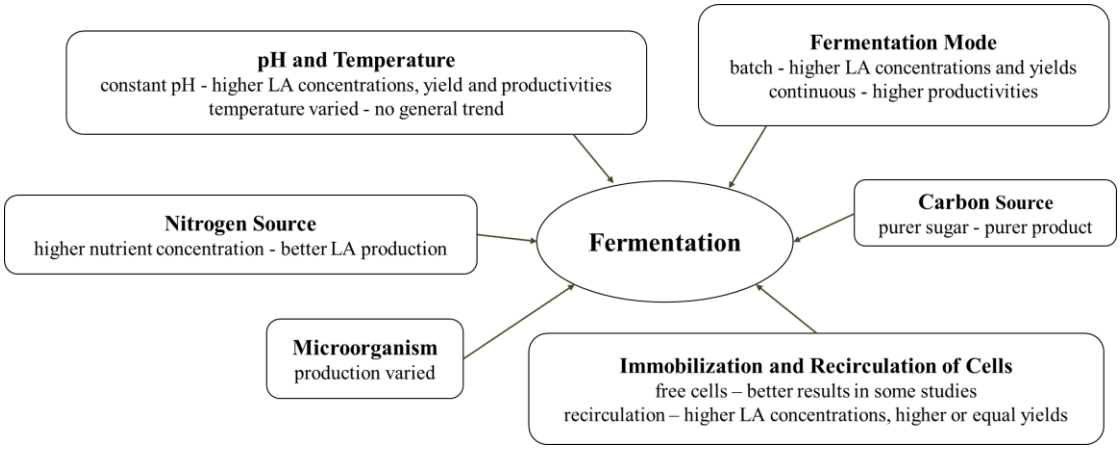

Figure 2.4 Parameters effecting LA production from fermentation processes.

To achieve good production, it is economically desirable to find the most favorable fermentation conditions. The effectiveness of a process can be measured as the concentration of LA produced, as the yield of LA based on substrate and as the productivity or LA production rate (Abdel-Rahman et al., 2013). As a result, much research work has focused on screening process parameters for biotechnological LA production. Generally, purer product is obtained with purer sugar fermented and higher nutrient concentration leads to better LA production (Komesu et al., 2017). In most of the studies, the batch fermentation mode gave a higher LA concentration and yield with all substrate utilized, whereas the continuous mode resulted in a higher productivity. Some of the studies showed that free cells gave better results, while the others suggested that recirculation of cells resulted in a higher LA concentration and higher or equal yield. In addition, titration to a constant pH produces a higher LA concentration, yield

and productivity, compared to leaving pH to decrease during LA fermentation (Hofvendahl & Hahn–Hägerdal, 2000).

However, there is no general trend of temperature impact applicable for most LAB yet. The effect of temperature on the production of LA from glucose has only been studied in a few reports, as shown in the references cited below.

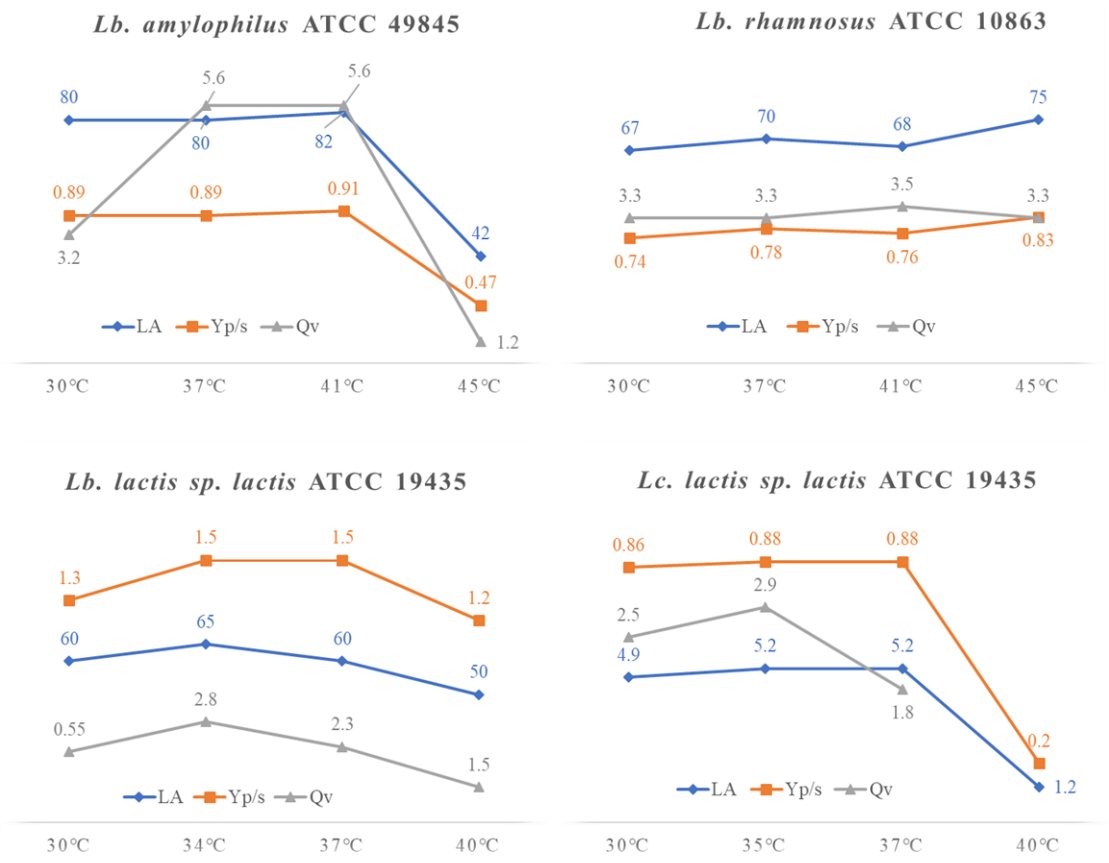

Figure 2.5 Influence of temperature on LA production from glucose (Yumoto & Ikeda, 1995; Hujanen& Linko, 1996; Hofvendahl, 1998; Åkerberg, Hofvendahl, Zacchi, & Hahn-Hägerdal, 1998).

LA: lactic acid concentration, g/L; $Y_{P/S}$: product yield, g/g; Q_V: volumetric lactic acid productivity, g/(L•h).

As shown in Fig 2.1, for *Lb. amylophilus*, the optimal temperatures were between 37 and 44°C for the maximum productivity and yield (Yumoto & Ikeda, 1995). For *Lb.*

rhamnosus and *Lc. lactis* exhibited the highest yield and productivity at 33 to 35°C and 41 to 45°C, respectively (Hujanen& Linko, 1996; Hofvendahl, 1998; Åkerberg, Hofvendahl, Zacchi, & Hahn-Hägerdal, 1998). We could see that in some cases the same temperature gave the best results in all categories, while the temperature resulting in the highest productivity was lower than the temperature giving highest LA concentration and yield in others. And the optimal temperature varied from different strains. Thus, detailed studies on the effects of temperature on cell growth, LA production and residual sugar during fermentation of LA from glucose by *L. pentosus* are still needed and will be performed in this study.

2.4 Kinetic modeling and LA fermentation

Mathematical models hold the key for engineering systems. Often a theory leads to mathematical formulations, and the validity of the theory is tested by comparing predicted responses to the ones in experiments (Motta & Pappalardo, 2012). In practice, the sustainable (or steady) state can be fluctuating with a noticeable degree, different from what is known or when no human interruption is imposed. A well-developed mathematical model gives bioprocess engineers an idea of what to expect by accurately predicting the dynamic outcomes and enhancing the ability to meet sustainability requirements (Liu, 2016).

To describe a microbial process, two kinds of models can be developed, structured and unstructured models. Compared to structured models, unstructured models are much easier to use, and have been proven to accurately describe LA fermentation in a

wide range of experimental conditions and media (Bouguettoucha, Balannec, & Amrane, 2011). In unstructured models, only total cellular concentration is considered, and hence they do not involve any physiological characterization of the cells (Rogers, Bramall, & McDonald, 1978).

A kinetic model can be used to predict the influence of fermentation operating parameters on cell growth, substrate utilization and LA production, providing a general understanding of the metabolic processes involved in LA production as well as the basis for better optimization strategies (Motta & Pappalardo, 2012). Such models can further be applied to cautiously predict the growth of organisms under conditions for which experiments have not yet been performed. That is they can provide useful and testable hypotheses and a mathematical framework to aid in interpreting results.

2.5 Using ^{1}HNMR to quantify compounds in fermentation broth

Traditionally, compounds in fermentation broth have been quantified chromatographically using high performance liquid chromatography (HPLC), gas chromatography (GC) or a related technique, and chemical structures have been identified with nuclear magnetic resonance (NMR) spectroscopy (Yang et al., 2016). However, recent studies have proven that a NMR technique can also be used to accurately quantify compounds like carbohydrates, organic acids and amino acids in both one dimension (proton NMR) and two dimensional (proton – carbon NMR). NMR can selectively detect most of the fermentation compounds in one prepared sample, unlike the chromatography methods (Holzgrabe, 2010). NMR quantification of

fermentation metabolites and substrates is made either by integration of NMR chemical shifts with the use of calibration references or by partial least-squares regression (Nord et al., 2004). When signals interfere with each other and result in partially overlapped or overlapped ^{1}H NMR spectrum, two dimensional ^{1}H-^{13}C Heteronuclear Single Quantum Correlation (HSQC) NMR technique can be used to avoid overlapping signals and accurately quantify individual monosaccharides (Rai & Chandel, 2015).

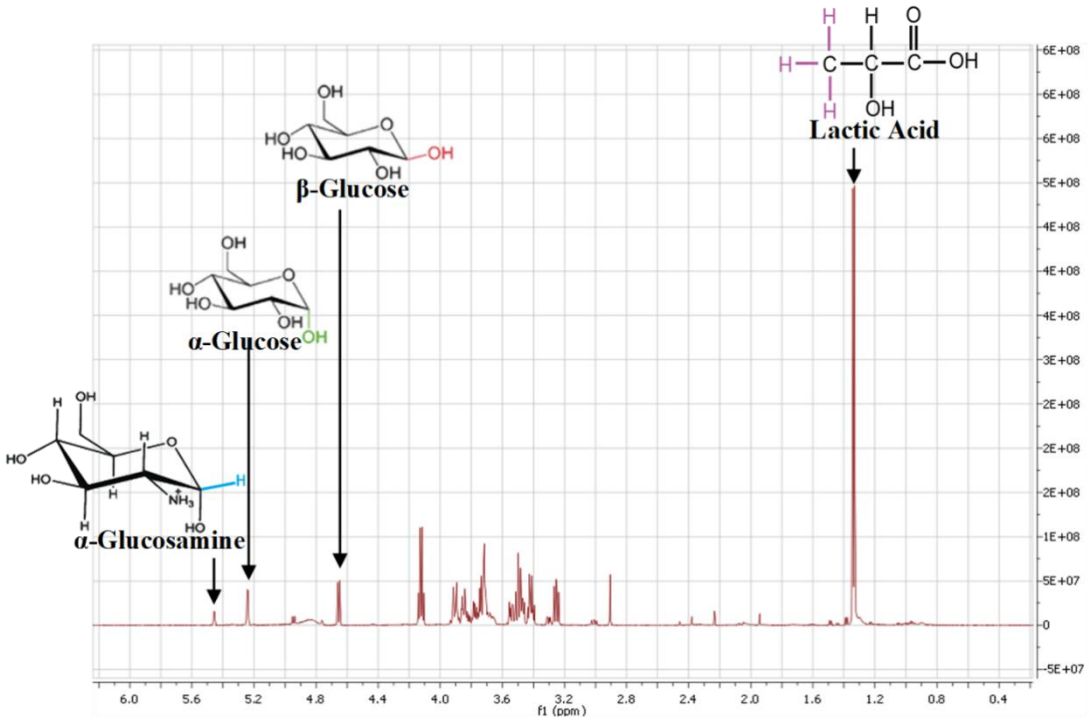

Figure 2.6 1D NMR for quantification of glucose and lactic acid by using glucosamine as the internal standard.

Fig 2.5 Shows the ^{1}H NMR spectrum of fermentation broth from batch fermentation. It can be observed that there is little interference among signals of the glucosamine internal standard, glucose and LA, the substrate and product of fermentation in this study. Therefore, ^{1}H NMR analysis can be performed well with careful manual integration for quantification of compounds in fermentation broth. The C1- α and C1- β anomeric protons are integrated and summed for glucose and a

reference standard of known mass concentration is used to determine the concentration of the glucose and LA.

2.6 Using optical density (OD) to quantify cell biomass in fermentation broth

Quantification of cell biomass in the fermentation broth is essential to determine the kinetics of microbial growth. In many cases, direct measurement is not feasible due to the presence of suspended solids or other interfering compounds in the medium (Zhang et al., 2009).

OD indicates the optical density or light absorbed by the object to be detected. When light passes through the microbial suspension, it will be partly scattered and partly absorbed by the cells and the amount of light transmitted will be reduced (Myers, Curtis & Curtis, 2013). Within a certain range, the transmittance decreases and the OD increases when the microbial cell concentration increases. However, the OD or transmittance is also affected by other factors, such as cell size, morphology, composition of the seed culture, and wavelength of light used (Griffiths et al., 2011). Therefore, the concentrations of bacterial suspensions can be measured only within a series of known OD of the same strain under the same conditions. The wavelength of light wave used is usually between 400 and 700 nm, depending on the microorganism concentration used, and the maximum absorption wavelength and stability of the cells (Stevenson et al., 2016). From the standard curve of OD value against cell concentration, the corresponding bacterial concentration can be determined by plotting the measured OD of the sample solution. The OD method has the advantages of being simple, rapid,

non-intrusive, and good for continuously measurement, which is beneficial for automatic control.

2.7 Previous kinetic study of LA production by *L. pentosus*

In Buyondo's research, *Lactobacillus pentosus* ATCC 8041, the same LAB strain used in this study, had been successfully adapted and used in concentrated wood extract hydrolysate in order to obtain a high LA yield via batch and continuous fermentation processes. In the batch fermentation at 37 ℃ and pH 6.0, lower total sugar concentration led to the highest product yield of 0.83 g/g. It was observed that acetic acid was the main by product and its production started after depletion of hexose. In the continuous fermentation process, a higher LA productivity of 2.36 g/(L·h) was obtained, compared to the productivity of 1.53 g/(L·h) obtained in batch process. Taking end product inhibition into account, an unstructured kinetic model was developed to describe biomass growth, product formation and substrate utilization in batch LA production from sugar maple wood hemicelluloses (Buyondo & Liu, 2011).

2.8 Summary

Lactic acid is mainly obtained from fermentative production. However, there are limited studies on the temperature effects during the fermentation process, especially the optimal temperature for one particular LAB strain. Therefore, the aims of this study were to study the temperature effects on the cell growth of *L. pentosus*, glucose utilization and LA production during batch fermentation process, and to develop a kinetic model to simulate the process.

CHAPTER 3: MATERIALS AND METHODS

The experimental flow chart is shown in Fig 3.1. The activated microorganism was processed into batch fermentation with variable temperatures. Collected samples were subjected to NMR spectroscopy and the OD standard curve to figure out the optimal temperature for cell growth, LA production and glucose utilization. A verification experiment of pH effects was then conducted to validate the optimal temperature. At last, an unstructured kinetic model was developed to simulate the batch fermentation process.

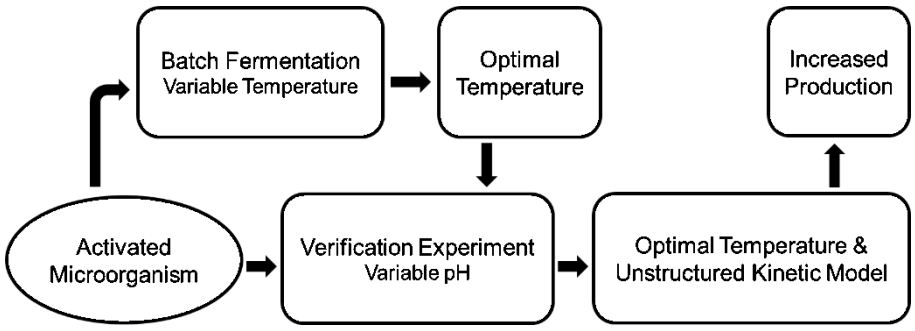

Figure 3.1 Experimental flow chart of continuous fermentation.

3.1 Seed culture preparation

The bacterial strain *L. pentosus* ATCC 8041 used was obtained from the American Type Culture Collection (ATCC). The strain was maintained on MRS agar medium slant and stored at 4 °C. The strain was transferred every 3 - 4 weeks to a fresh medium. The MRS medium was made as: 10.0 g/L proteose peptone 3, 10.0 g/L beef extract, 5.0 g/L yeast extract, 20.0 g/L dextrose, 1.0 mL/L Tween 80, 2.0 g/L ammonium citrate, 0.1 g/L $MgSO_4$, 0.05 g/L $MnSO_4$, 2.0 g/L K_2HPO_4 and 5.0 g/L CH_3COONa and supplemented with 20 g/L agar to make slant. All medium components were purchased

from Fisher Scientific, Pittsburgh, PA, USA. The seed culture was prepared by picking 1 - 2 big colonies from the slant and inoculating them into 100 mL MRS medium contained in 250 mL screw capped plastic flasks (NALGENE, Rochester, NY, USA). The seed culture was incubated at 37 °C for 20 - 24 h on a rotary shaker (GYROMAXTM 747R, Amerex Instruments, Lafayette, CA, USA), operating at 150 rounds per minute (rpm).

3.2 Batch fermentation process

Batch fermentation experiments were conducted in a 1.0 L New Brunswick Bioreactor (BIOFLO 110; New Brunswick Scientific Co., Edison, NJ, USA) with 800 mL working volume. The fermentation medium contained 65 g/L glucose, 10 g/L yeast extract, 2 g/L K_2HPO_4, 2 g/L KH_2PO_4 and 0.5% (v/v) Tween 80. All medium components were purchased from Fisher Scientific, Pittsburgh, PA, USA. The bioreactor was inoculated with 5 mL of centrifugation concentrated actively growing 20 to 24 hour-old seed culture. The pH of medium was adjusted to and maintained at 6.0 by the addition of 5 mol/L NaOH prior to inoculation and during fermentation. Agitation speed was set at 150 rounds per minute (rpm) and air flow rate at 25 mL/min. Temperatures studied were carried out at 20 ℃, 25 ℃, 28 ℃, 30 ℃, 35 ℃, 37 ℃, 40 ℃, 42 ℃ and 45 ℃. Batch fermentations with pH at 5.0, 6.0, 7.0 and 8.0 were then conducted at the obtained optimal temperature to verify the temperature effects (agitation speed at 150 rpm and air flow rate at 25 mL/min). Samples (2 mL) were taken at given fermentation time intervals and centrifuged at 4000 rpm for 5 min. The

supernatants were stored at -10 ℃ for LA and glucose analyses. Experimental data were obtained in triplicates.

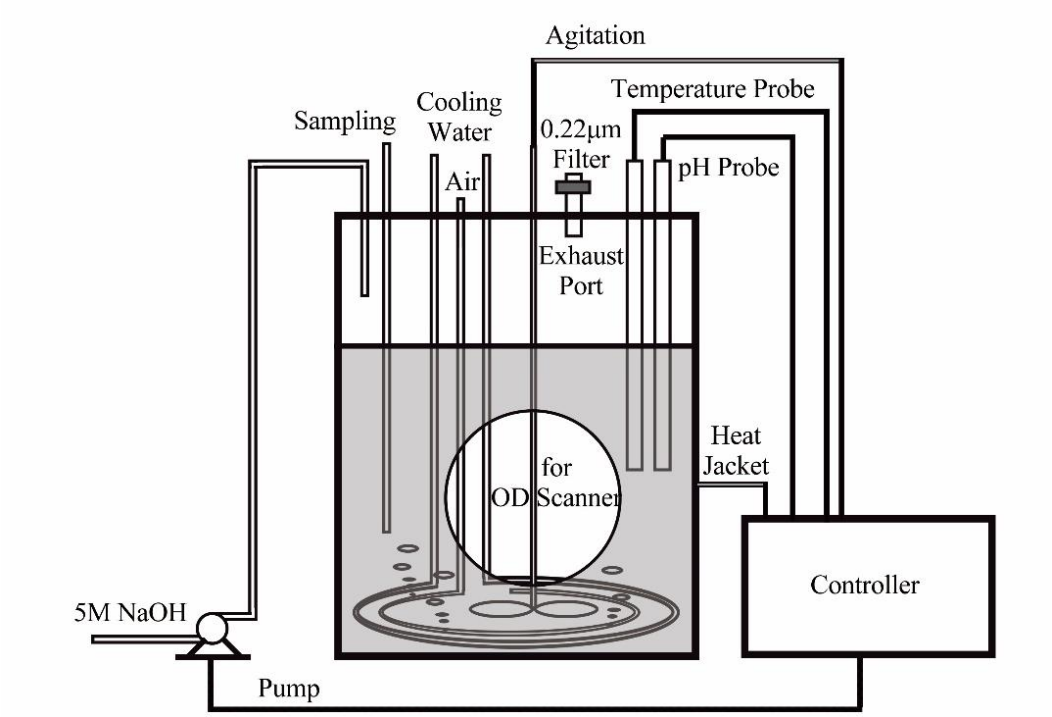

Figure 3.2 Schematic diagram of batch fermentation system in this study.

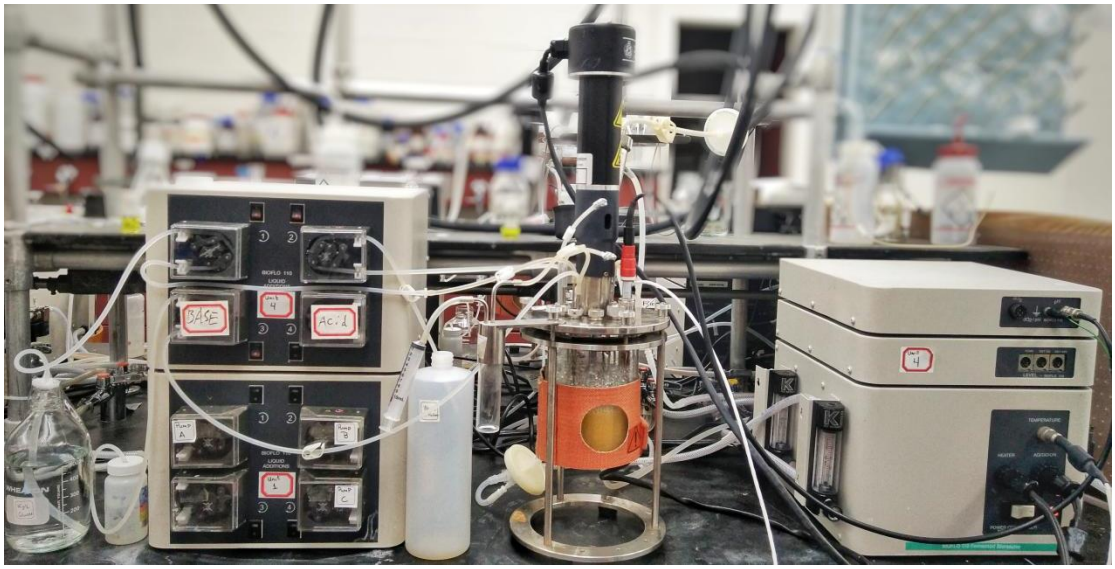

Figure 3.3 The bioreactor used for LA fermentation located at lab 204 of department of Paper and Bioprocess Engineering, SUNY-ESF.

3.3 Determination of substrate and product concentrations

Samples were prepared by mixing 0.1 mL sample, 0.1 mL internal standard (95.6 % wt deuterium oxide, 4.2% wt glucosamine, 0.2 % wt trimethylamine and 0.1% wt trimethylsilyl propionate) and 0.8 mL deuterium oxide (Acros organics) in a 5-mm-o.d. NMR tube (Corning, NY, USA). Standard solutions of LA and glucose with known ranges of concentrations were subjected to ^{1}HNMR spectroscopy and respective calibration curves of normalized peak area against concentration were generated (Appendix A, a & b).

Figure 3.4 The NMR tubes used for determination of substrate and product concentrations stored at lab 204 of department of Paper and Bioprocess Engineering, SUNY-ESF.

The α-glucosamine signal peak area was used as the reference for quantification of analytes whereas trimethylsilyl propionate (TSP) was set as the reference point at 0 ppm chemical shift. LA, α-glucose and β-glucose methyl group signals located at 1.31 – 1.36 ppm, 5.26 – 5.22 ppm and 4.68 – 4.82 ppm, respectively were used for quantification of analytes. The peaks were integrated using MestReNova software and normalized to C1-α anomeric peak for glucosamine. Concentrations of individual analytes were determined by comparing the obtained peak area to the respective calibration curve.

3.4 Determination of cell biomass concentration

The cell biomass concentration was determined by measuring the optical density (OD) using an OD scanner (BugLab, CA, USA). As the standard curve provided by the scanner was for *E. coli*, a standard curve of *L. pentosus* was needed and it was developed by obtaining the dry weight of samples with known *E. coli* OD values. A pre-weighed beaker containing 50 mL of sample was air-dried in the oven at 80 ℃ to constant weight. The cell mass of the respective samples was defined as the difference in the measured weights of the beaker before and after drying. Concentration of biomass analytes was determined by comparing the obtained OD reading to the calibration curve (Appendix A, c).

Figure 3.5 The OD scanner used for determination of cell biomass concentration located at lab 204 of department of Paper and Bioprocess Engineering, SUNY-ESF.

3.5 Kinetic modeling

Several assumptions and possible models were evaluated based on the experimental data and observations. Estimation was then conducted to verify those showing the potential. To estimate kinetic parameters, it was required to search for values at which predicted data of the glucose concentration, biomass concentration, and LA concentration were close to the experimental data, within acceptable tolerance, during the whole fermentation process. Kinetic parameters were determined by simultaneously solving the equations for the dependent variables, glucose concentration, biomass concentration, and LA concentration, using ODEXLIMS function developed in Excel (Liu, 2013). The best fitting parameters were determined by using Excel solver to minimize the variance between the predicted and the experimental data.

CHAPTER 4 RESULTS AND DISCUSSION

This chapter discusses the results and findings gathered in this study, including the kinetics study of glucose utilization and LA production by *L. pentosus* in the batch fermentation process with a focus on the effects of temperature and pH on the cell growth of *L. pentosus*, utilization of glucose and production of LA. An unstructured mathematical kinetic modeling of *L. pentosus* cell growth rate, product formation rate and glucose utilization rate was developed.

4.1 Temperature effects on LA batch fermentation by *L. pentosus* from glucose

The batch reactor is an idealized reactor, without inlets or outlets. The reaction mixture is assumed to be well-mixed at all times in the batch reactor (Fogler & Brown, 1992). Therefore, the temperature and concentration are uniform inside the reactor at any given time, which makes its analysis far simpler.

Concentrated *L. pentosus* seed culture (5 mL) was inoculated into the prepared fermentation medium and set to run for 60 hours. To investigate the possible effects of temperature, batch fermentations were carried out at variable temperatures (20 ℃, 25 ℃, 28 ℃, 30 ℃, 35 ℃, 37 ℃, 40 ℃, 42 ℃ and 45 ℃) while all the other process parameters remained the same (pH 6.0, agitation speed at 150 rpm and air flow rate at 25 mL/min). Figs 4.1 to 4.3 are the profiles of glucose utilization, LA production and cell growth during batch fermentation at different temperatures (pH 6.0, agitation speed at 150 rpm and air flow rate at 25 mL/min), respectively. Concentrations of glucose, LA and biomass were shown with fermentation time. Triplicate of independent runs

were performed for each set of parameters. Fig 4.1 shows both the trend and the error bar of glucose, cell biomass and LA concentration as function of time.

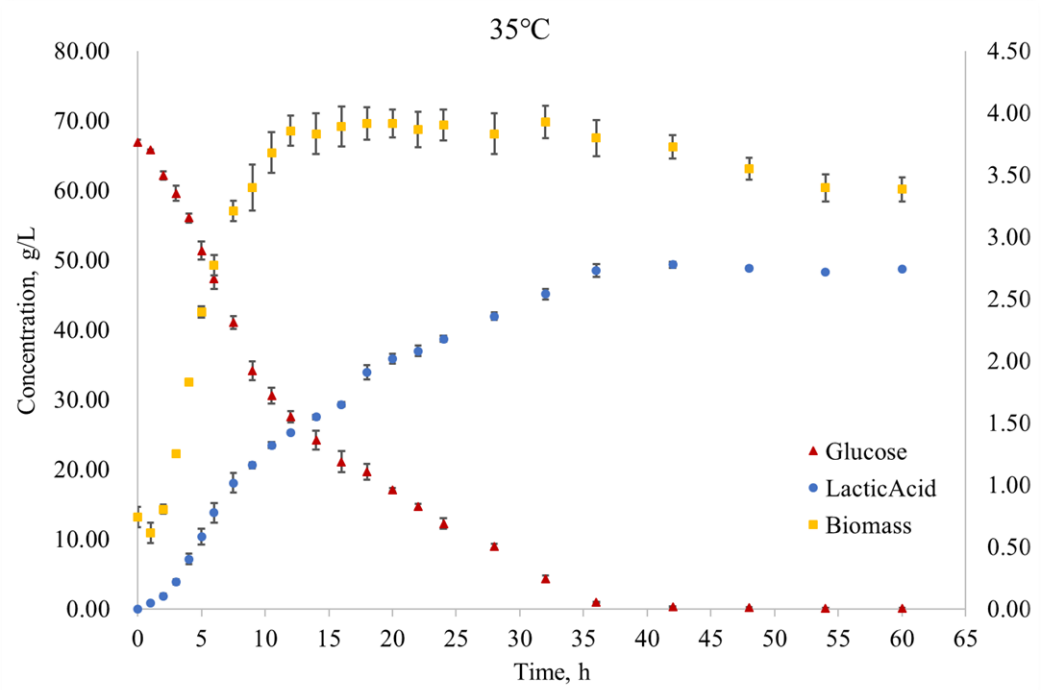

Figure 4.1 Profiles of glucose utilization, biomass growth and LA production during batch fermentation at 35 ℃ (pH 6.0, agitation speed at 150 rpm, and air flow rate 25 mL/min). Standard error was obtained from the triplicate independent experiments and included as above.

4.1.1 Glucose utilization

As shown in Fig 4.2, glucose concentration decreased with time and glucose was consumed rapidly within the first 35 hours, gradually approaching steady state. Shown in Fig 4.3, in the batches at 28 ℃, 30 ℃, 35 ℃, 37 ℃ and 40 ℃, the maximum glucose consumption was at a similar rate within the first 35 hours and glucose was almost completely consumed after 60 hours with less than 1.70 % of residual glucose (Appendix D). In the batches at 20 ℃, 25 ℃, 42 ℃ and 45 ℃, glucose utilization was at a slower rate and a considerable amount, up to 44.00 % of glucose remained unconsumed after 60 hours. Among all the batches, glucose was utilized most

thoroughly at 35 ℃, with the highest maximum glucose consumption rate of 4.24 h^{-1} and the lowest residual glucose concentration of 0.17%.

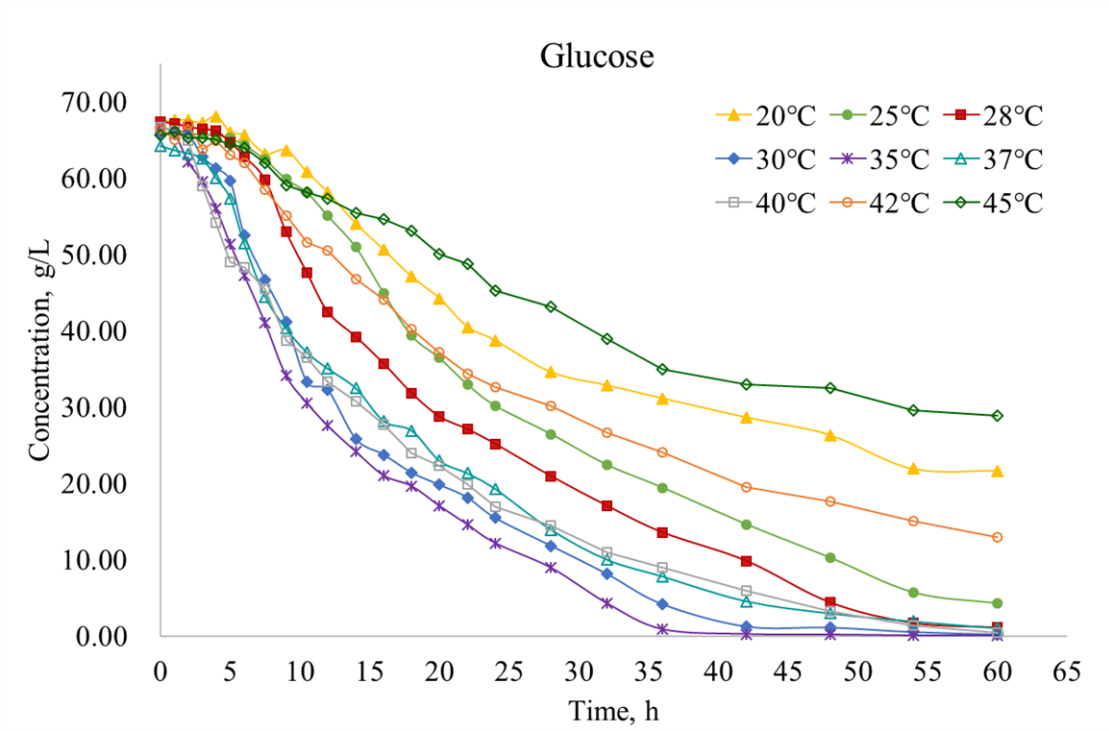

Figure 4.2 Sugar utilization profiles during batch fermentation at different temperatures (pH 6.0, agitation speed at 150 rpm, and air flow rate 25 mL/min).

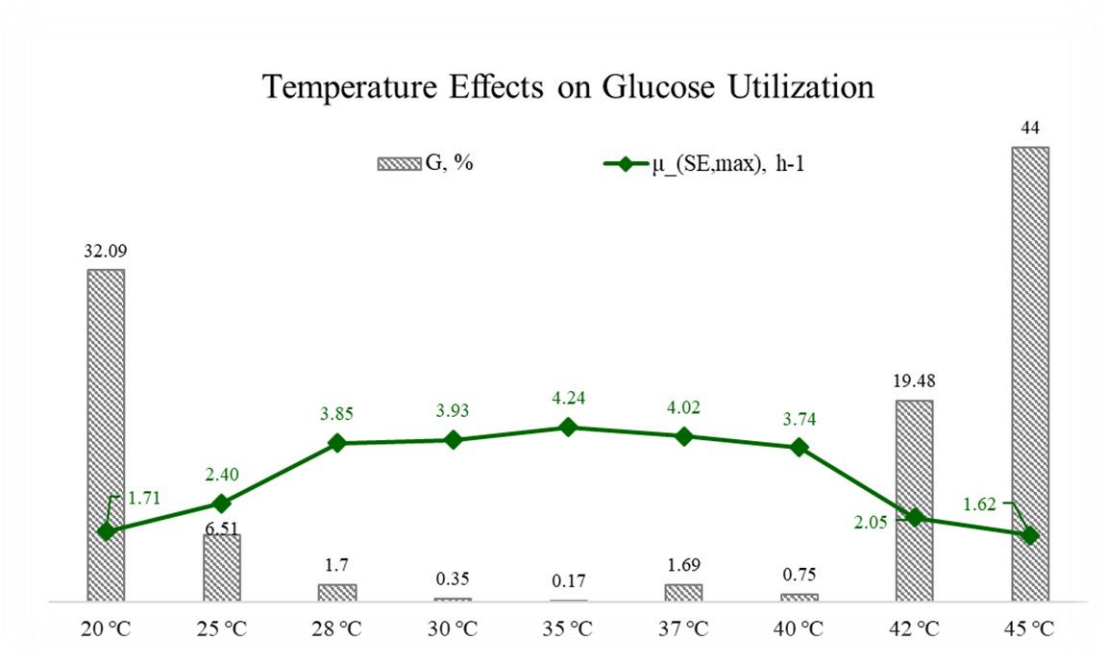

Figure 4.3 Influence of temperature on the glucose utilization during batch fermentation (pH 6.0,

agitation speed at 150 rpm, and air flow rate at 25 mL/min).

T: temperature, degrees Celsius; G: residual glucose concentration, percentage of initial glucose concentration; μ_(SE,max): maximum glucose consumption rate obtained from experiment, per hour.

Therefore, it can be inferred that the glucose utilization rate increases when the temperature increases from 20 ℃ to 35 ℃ but decreases when the temperature increases from 35 ℃ to 45 ℃. On the other hand, the residual glucose decreases with the temperature from 20 ℃ to 35 ℃ but increases with the temperature from 35 ℃ to 45 ℃. The optimal temperature for glucose utilization is likely to be 35 ℃, based on glucose consumption rate and lowest residual glucose after 60 hours.

4.1.2 Biomass growth

A typical batch growth curve includes the following phases: (1) lag phase, (2) logarithmic or exponential growth phase, (3) deceleration phase, (4) stationary phase and (5) death phase (Zwietering et al., 1990). Shown in Fig 4.4, the biomass concentration experienced a slight decrease within the first 5 hours, which was the lag phase of cell growth, and then increased rapidly, which was the exponential growth phase. In contrast to standard growth curves, the deceleration phase of *L. pentosus* growth under the batch fermentation conditions in this study (20-40 ℃, pH 6.0) was not apparent expect the batches at 42 ℃ and 45 ℃. Because under those temperatures, the low enzyme activity made the period of cell growth longer. After reaching the stationary phase, it appeared to fluctuate within a certain range during the rest of the fermentation.

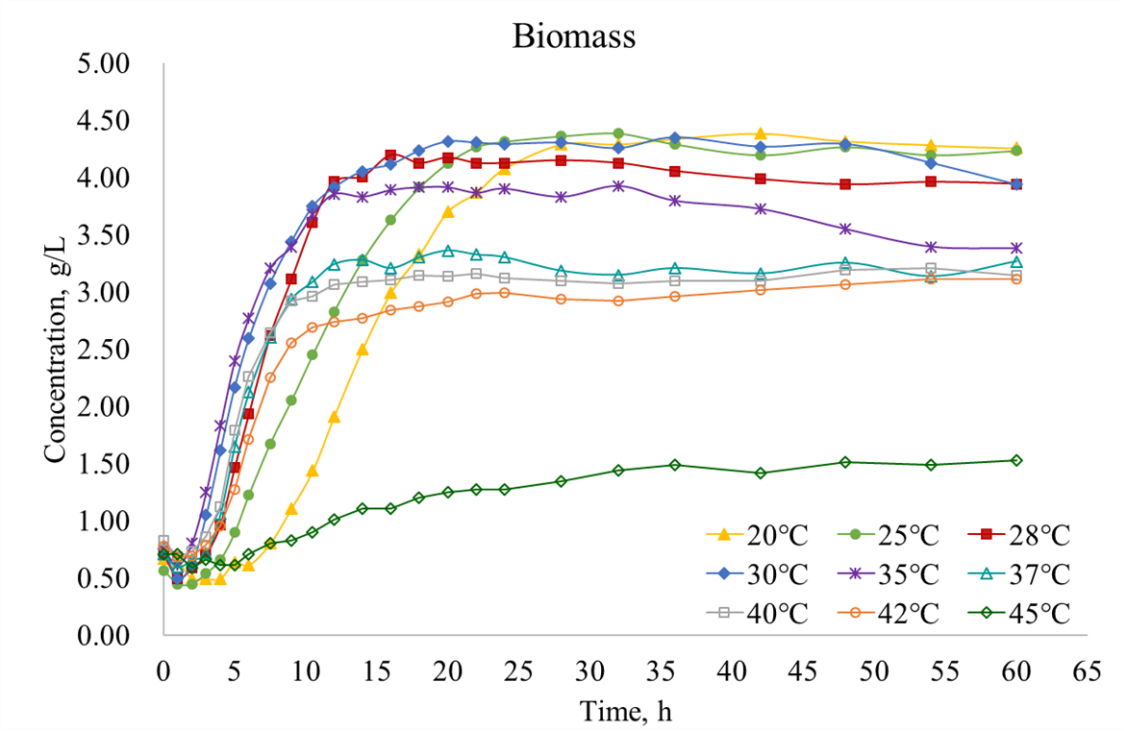

Figure 4.4 Biomass growth profiles during batch fermentation at different temperatures (pH 6.0, agitation speed at 150 rpm, and air flow rate at 25 mL/min).

The lag phase occurs immediately after inoculation, as a period of *L. pentosus* adaptation to the new environment. The concentration of nutrients, growth factors and the age of the inoculum culture have strong effects on the length of the lag phase. Multiple lag phases may be observed when more than one carbon source can be accessed from the medium (Rolfe et al., 2012). In this study, the same formula was used to prepare the fermentation broth and the same length of culture time was applied to activate the cells. The fermentation broth contains a single carbon source which is glucose. The microorganism was processed into different mediums during the seed culture preparation and fermentation. Thus, there was only one lag phase as shown on the cell growth curve right after inoculum. The length of the lag phase of cell growth reflects on how well adapted the growth factors are for the organism. Shown in Fig 4.5,

in the batches at 20 ℃, 25 ℃, 28 ℃, 30 ℃ and 35 ℃, it took a shorter period of time for biomass concentration to start growing, and the opposite tendency could be found in the batches at 37 ℃, 40 ℃, 42 ℃ and 45 ℃ with a longer lag phase, which suggests that the lag phase tended to be shorter as temperature increased from 20 ℃ to 35 ℃ and then, became longer as temperature increased from 35 ℃ to 45 ℃.

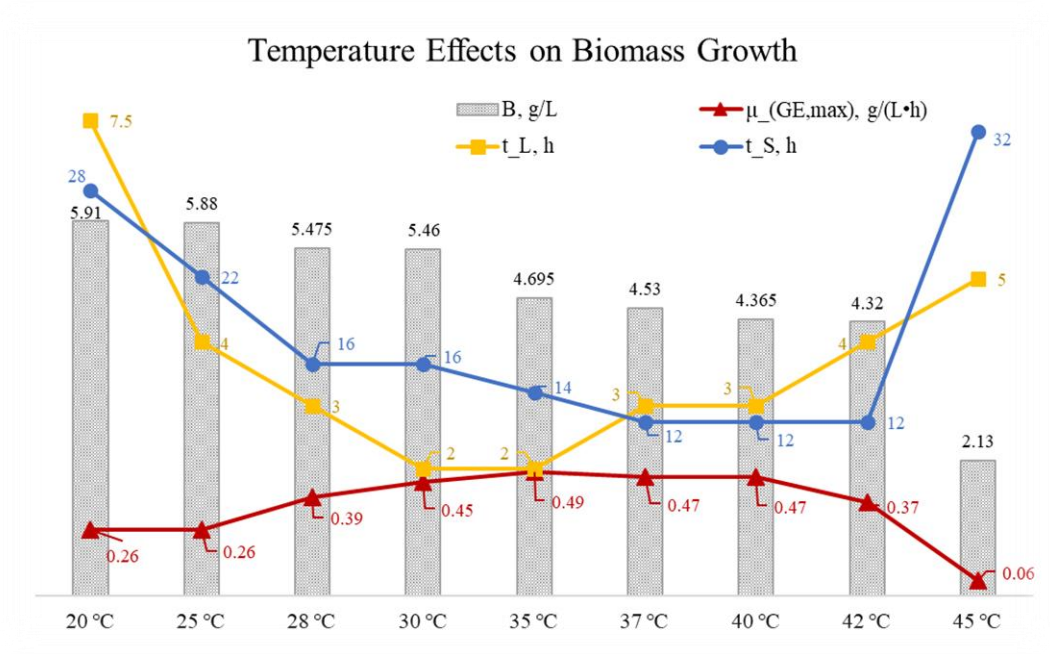

Figure 4.5 Influence of temperature on the biomass growth during batch fermentation (pH 6.0, agitation speed at 150 rpm, and air flow rate at 25 mL/min).

T: temperature, degrees Celsius; B: biomass concentration, gram per liter; μ_(GE,max) maximum biomass growth rate obtained from experiment, per hour; t_L, time period of lag phase, hour; t_S, time required to reach stationary phase, hour.

The maximum growth phase, also known as the exponential growth phase or logarithmic growth phase, follows the lag phase. In this phase, cells can multiply rapidly at a maximum rate, and cell mass and cell number density increase exponentially with time (Maier & Pepper, 2015). In the batches at 28 ℃, 30 ℃, 35 ℃, 37 ℃, 40 ℃ and 42 ℃, the maximum growth phase happened within the first 15 hours

and it extended to 25 hours at 20 ℃, 25 ℃ and 45 ℃. The highest maximum growth rate of biomass was obtained as 0.49 g/(L·h) at 35 ℃, followed by 30 ℃, 37 ℃, 40 ℃, 28 ℃, 42 ℃, 25 ℃, 20 ℃ and 45 ℃ (Appendix E), suggesting that the cell growth rate rose when the temperature increased from 20 ℃ to 35 ℃ but dropped when the temperature increased from 35 ℃ to 45 ℃.

During the stationary phase, the net growth rate is zero (growth rate is equal to the death rate) and the total cell mass concentration may stay constant, but the number of viable cells may decrease and the cell lysis may occur. Cells may grow on lysis products of lysed cells, when a second growth phase may occur (Newton, 2018). In all the batches, the cell biomass concentration stopped growing much earlier than the glucose was all consumed. It was because the fermentation broth contained abundant amount of carbon source, which was glucose, as the substrate for LA production, but a limited amount of nitrogen source, to lower the cell growth and improve the product yield.

At the end of the stationary phase, the death phase begins due to nutrient depletion. However, a clear demarcation between them is not always possible as some cell death starts during or even before the stationary phase (Mason & Egli, 1993). In the batches at 30 ℃ and 35 ℃, glucose was almost gone after 40 hours so that the cell mass concentration began to decrease markedly. In the rest of the batch fermentation, since there was a quite large amount of residual glucose, the cell growth was still at the stationary phase. After 60 hours of the fermentation, the batch fermentation at 20 ℃ had the highest biomass concentration of 3.94 g/L, followed by 35 ℃, 28 ℃, 30 ℃, 35 ℃, 37 ℃, 40 ℃, 42 ℃ and 45 ℃, which indicated that the biomass concentration

at stationary phase decreased when the fermentation temperature increased.

4.1.3 LA production

In Fig 4.6, the LA production followed the same trend as the glucose utilization, increasing rapidly during the first 35 hours and gradually reaching the steady state afterwards. Although *L. pentosus* is capable of metabolizing both 5-carbon and 6-carbon sugars, producing acetic acid from 5-carbon sugars as the main by-product (Buyondo & Liu, 2011), the fermentation medium in this study only contained glucose, a 6-carbon sugar. Theoretically, no significant acetic acid production was expected to be detected. In fact, there was no significant production of either acetic acid or ethanol in all batches. Therefore, it can be inferred that LA production by *L. pentosus* from glucose follows the EMP pathway only.

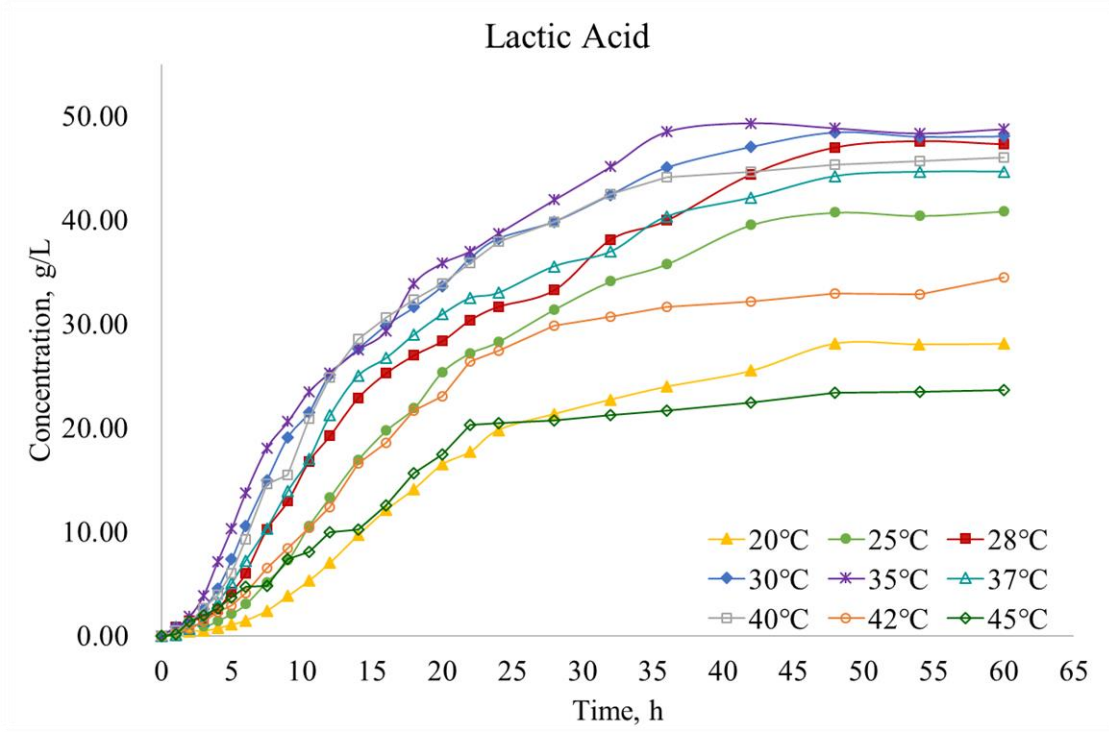

Figure 4.6 LA production profiles during batch fermentation at different temperatures (pH 6.0, agitation speed at 150 rpm, and air flow rate at 25 mL/min).

Shown in Fig 4.7, in the batches at 20 ℃, 25 ℃, 28 ℃, 30 ℃ and 35 ℃, the maximum LA formation rate rose from 1.13 h^{-1} to 3.15 h^{-1}, whereas in the batches at 37 ℃, 42 ℃ and 45 ℃, the maximum LA formation rate dropped to 1.35 h^{-1} (Appendix F). However, in the batch at 40 ℃, LA was produced at a higher speed than 37 ℃. It was because they shared the similar glucose utilization rate but less biomass was obtained in the batch at 40 ℃, showing that a lower proportion of carbon source was used for biomass growth at 40 ℃ thus a higher proportion for LA production. In all the batches, the fermentation time required to reach steady state was decreasing with temperature increasing. The batch fermentation at 35 ℃ had the highest maximum LA formation rate of 3.15 h^{-1} and the highest LA concentration of 48.75 g/L after 60 hours of the fermentation, followed by 30 ℃, 28 ℃, 40 ℃, 37 ℃, 25 ℃, 42 ℃, 45 ℃ and 20℃.

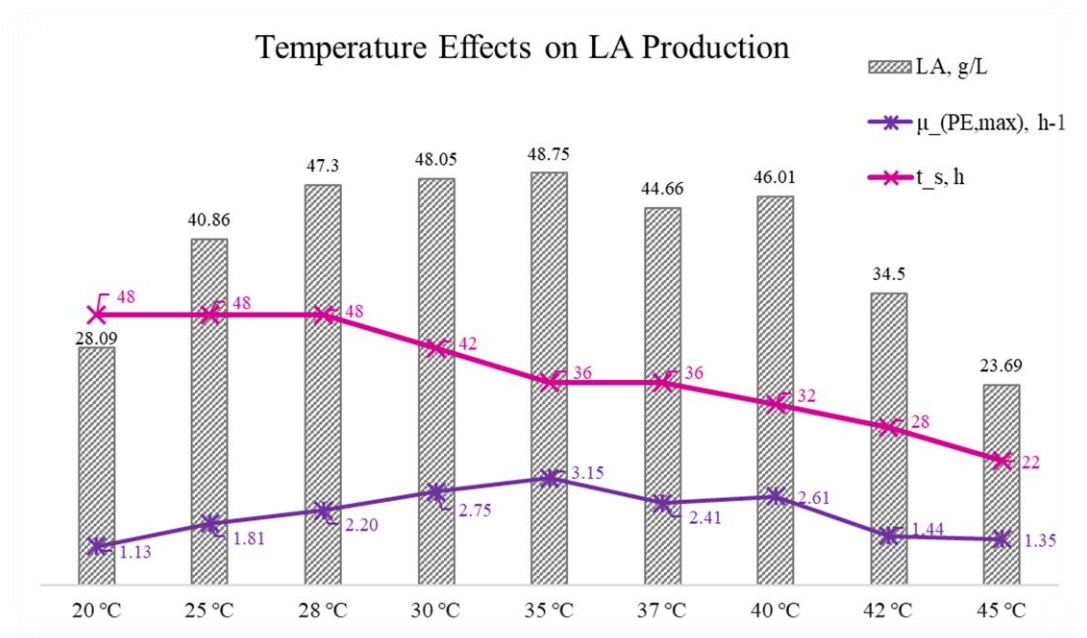

Figure 4.7 Influence of temperature on the LA production during batch fermentation (pH 6.0, agitation speed at 150 rpm, and air flow rate at 25 mL/min).

T: temperature, degrees Celsius; LA: lactic acid concentration, gram per liter; μ_(PE,max): maximum

LA formation rate obtained from experiment, per hour; t_s, time required to reach steady state, hour.

Therefore, it can be inferred that the LA production rate and the obtained LA concentration increase when the temperature increases from 20 ℃ to 35 ℃ but decreases when temperature increases from 35 ℃ to 45 ℃. The optimal temperature of LA production was shown to be 35 ℃. It was also observed that the fermentation time required to reach steady state decreases as the temperature increases from 20 ℃ to 45 ℃.

4.1.4 Temperature effects and the optimal temperature (pH 6.0)

Based on the above results, lower temperatures lead to better cell growth while higher temperatures result in more efficient glucose utilization and more productive LA generation (Fig 4.8). As the temperature increases from 20 ℃ to 35 ℃, glucose is utilized faster and more fully, contributing to a shorter lag phase in cell growth and producing more LA with a higher productivity and a higher product yield. However, when the temperature increases from 35 ℃ to 45 ℃, the glucose utilization slows down and more glucose remains unconsumed after 60 hours, extending the cell growth lag phase and generating less LA with a lower productivity and product yield. In addition, the obtained biomass concentration and the fermentation time required to reach steady state decrease with the temperature from 20 ℃ to 45 ℃.

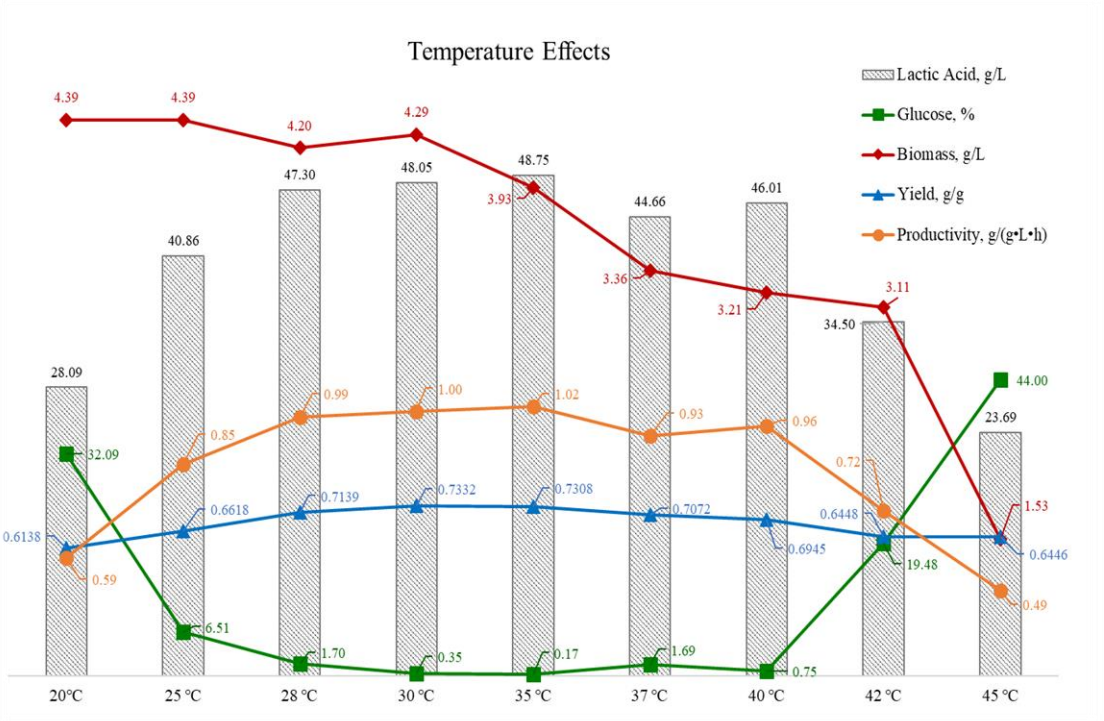

Figure 4.8 Influence of temperature on the biomass growth, LA production and glucose utilization during batch fermentation (pH 6.0, agitation speed at 150 rpm, and air flow rate at 25 mL/min).

From the data, it is apparent that 35 ℃ was the turning point of glucose utilization, biomass growth and LA production of the batch fermentation at pH value of 6.0. Although the batch fermentation at 30 ℃ and 37 ℃ both shared the approximate trends and outcomes of the glucose utilization, biomass growth and LA production with 35 ℃ and even more biomass was cultured at 30 ℃, the batch fermentation at 35 ℃ generated most LA at the fastest metabolic rate. This is a consequence of lower glucose utilization for biomass growth leaving more for LA production. After 60 hours of fermentation at 35 ℃, glucose was completely utilized, producing the highest LA concentration of 48.75 g/L, with the highest product yield of 0.7308 gram LA per gram consumed glucose and the highest productivity of 1.02 gram LA per gram consumed glucose per liter per hour (Appendix I). It can be concluded that 35 ℃ is the optimal temperature

during batch fermentation by *Lb. pentosus* from glucose (pH 6.0, agitation speed at 150 rpm, and air flow rate at 25 mL/min).

4.1.5 Verification experiment of pH effects on glucose utilization, biomass growth and LA production

To verify the validity of the conclusions above, the optimum pH value at a controlled temperature (35℃) for batch fermentation was determined by verification testing. Variable pH values (pH 5.0, pH 6.0, pH 7.0 and pH 8.0) were chosen and all the other process parameters remained the same (agitation speed at 150 rpm and air flow rate 25 mL/min). Fig 4.9 to 4.11 are the profiles of the glucose utilization, LA production and cell growth during batch fermentation at different pH (temperature at 35 ℃, agitation speed at 150 rpm and air flow rate at 25 mL/min), respectively. Concentrations of glucose, LA and biomass were showed with fermentation time.

Observed from Fig 4.9 to 4.12, the fermentation of pH 6.0 had the best glucose utilization, the highest productivity of LA and the highest growth rate of biomass at the exponential growth phase. In accordance with Fig 4.2, 4.4 and 4.7, glucose utilization, biomass growth and LA production curves in Fig 4.9 to 4.11 showed trends similar to the previous batches in the study of temperature effects. The time required for each concentration to reach its peak value was basically the same. Compared with the batch fermentation of 35 ℃ and pH 6.0 in the study of temperature effects, the relative errors (Appendix J) of glucose consumption and maximum biomass growth between these two groups of experiments were 4.6 % and 3.8 %, respectively. The above analysis showed that the experimental results were repeatable. Therefore, the verification testing

was effective. It validates that the optimal temperature is 35 ℃ when pH is 6.0 during batch fermentation by *L. pentosus* from glucose (agitation speed at 150 rpm, and air flow rate at 25 mL/min).

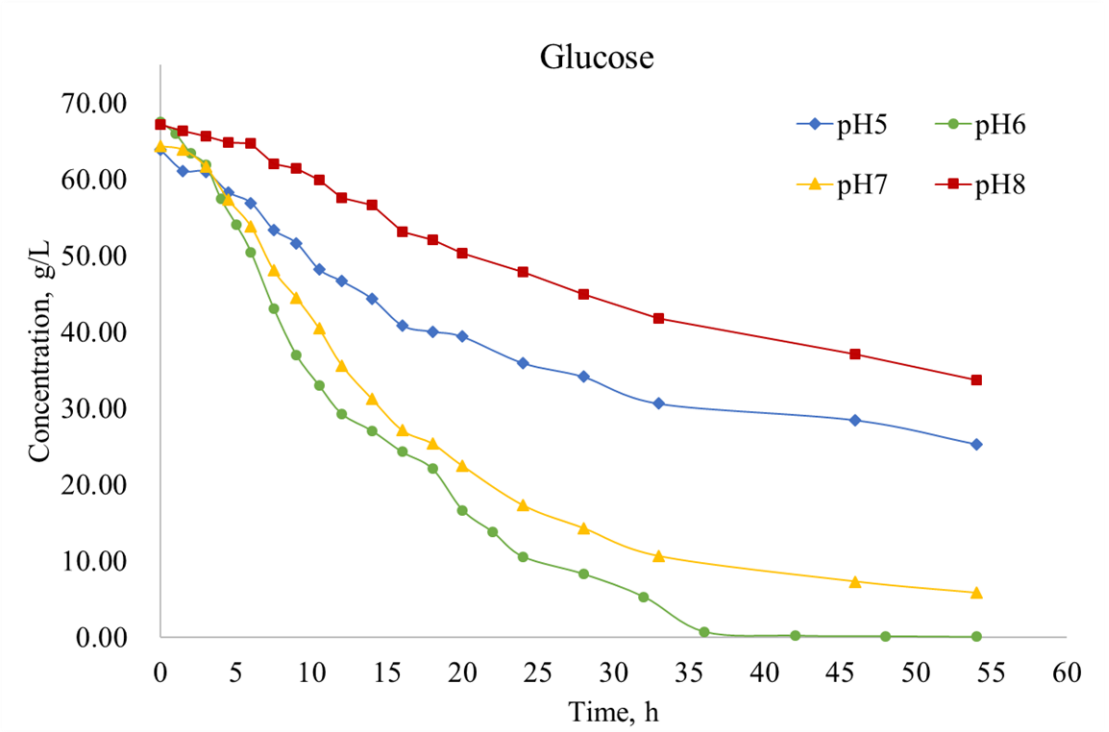

pH	5	6	7	8
G (%)	25.33	0.12	5.82	33.65

Figure 4.9 Glucose utilization profiles during batch fermentation at different pH (35 ℃, agitation speed at 150 rpm, and air flow rate at 25 mL/min) with residual glucose concentration at the end point.

G: residual glucose concentration, percentage of initial glucose concentration.

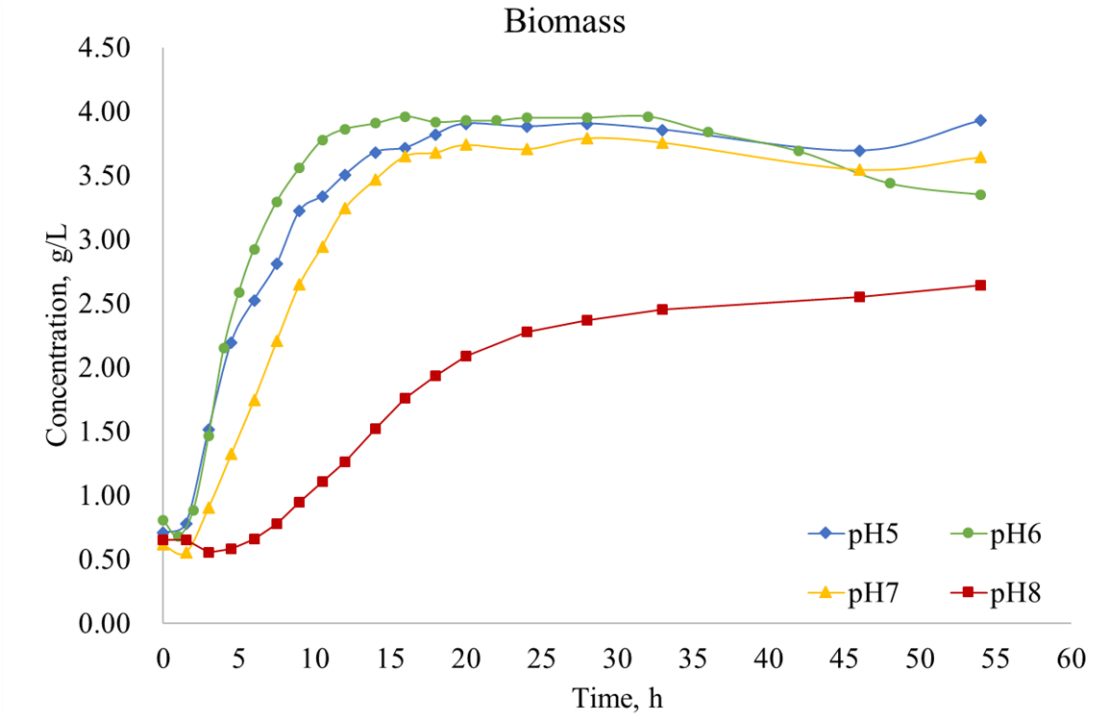

pH	5	6	7	8
B (g/L)	3.93	3.40	3.64	2.64

Figure 4.10 Biomass growth profiles during batch fermentation at different pH (35 °C, agitation speed at 150 rpm, and air flow rate at 25 mL/min) with biomass concentration at the end point.

B: biomass concentration, gram per liter.

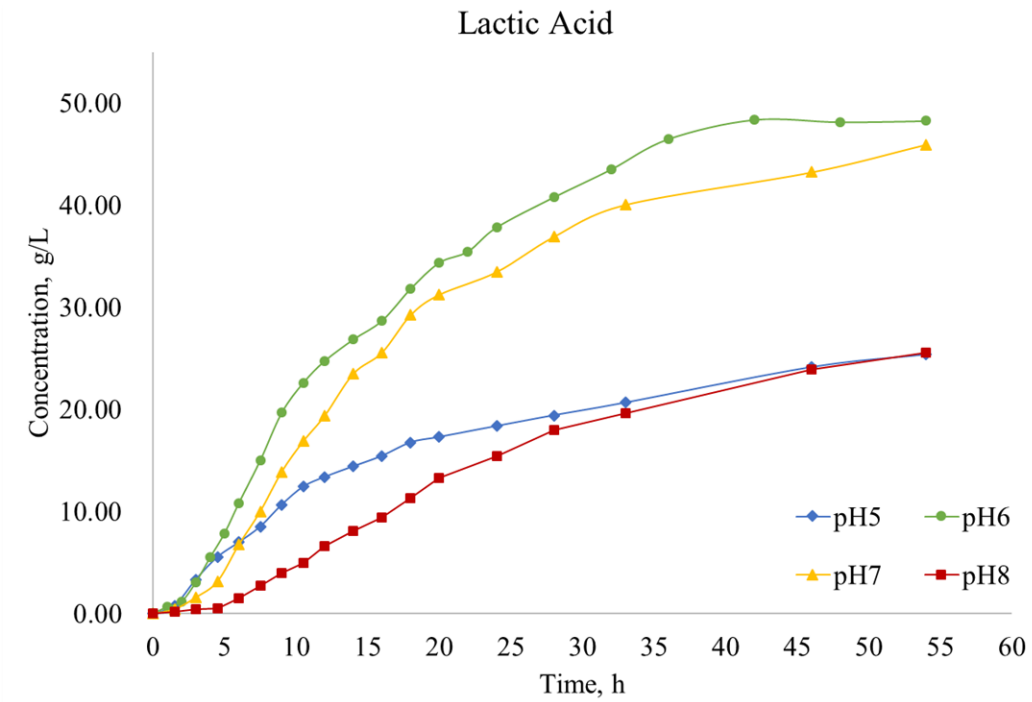

pH	5	6	7	8
LA (g/L)	25.37	48.33	45.93	25.58

Figure 4.11 LA production profiles during batch fermentation at different pH (temperature at 35 ℃, agitation speed at 150 rpm, and air flow rate at 25 mL/min) with LA concentration at the end point.

LA: lactic acid concentration, gram per liter.

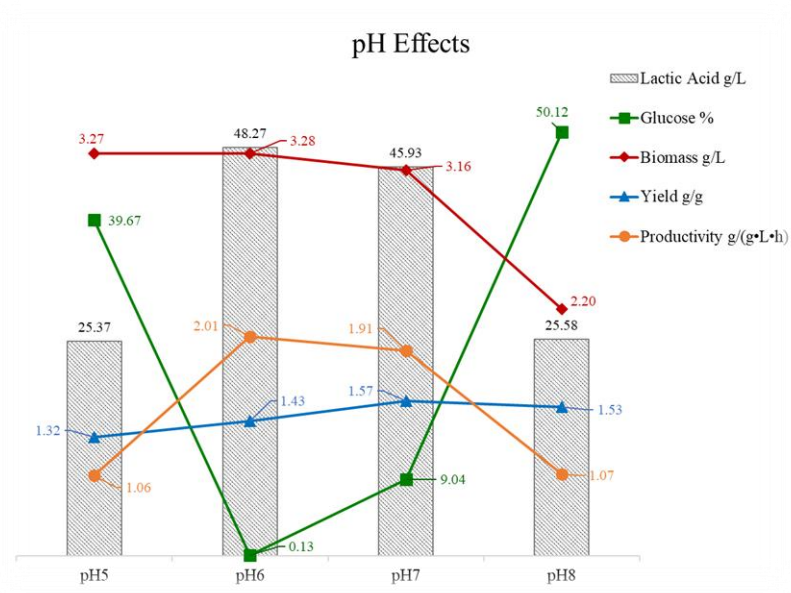

Figure 4.12 Influence of pH on the biomass growth, LA production and glucose utilization during batch fermentation (temperature at 35 ℃, agitation speed at 150 rpm, and air flow rate at 25 mL/min).

4.2 Unstructured kinetic modeling of LA batch fermentation from glucose

The experimental data obtained from batch fermentation at 35℃ and pH 6.0 were used to determine the kinetic parameters. An unstructured mathematical model was developed, with the capability of predicting cell growth, glucose utilization and LA production during batch fermentation at 35℃ and pH 6.0 from glucose by *L.pentosus*.

4.2.1 Mathematical model

During mathematical modeling, the following assumptions were made:

1. The batch reactor was well-mixed and the concentration in the reactor was consistent.

2. Carbon source and nitrogen source were the only two nutrients that limited cell growth.

Mass balance of the cell biomass in the batch reactor leads to:

$$0 - 0 + r_X V = \frac{d(XV)}{dt} \tag{4.1}$$

where r_X is the cell biomass growth rate, g/(L•h); X is the cell biomass concentration, g/L; t is the fermentation time; V is the reactor volume, L.

Mass balance of the limiting substrate in the batch reactor leads to:

$$0 - 0 + r_S V = \frac{d(SV)}{dt} \tag{4.2}$$

where r_S is the substrate reaction rate, g/(L•h).

Mass balance of the product in the batch reactor leads to:

$$0 - 0 + r_P V = \frac{d(PV)}{dt} \tag{4.3}$$

where r_P is the substrate reaction rate, g/(L•h).

Rate law for biomass (Juliastuti et al., 2003) is usually expressed as:

$$r_X = \mu_{net} X = (\mu_G - k_d) X \tag{4.4}$$

where μ_{net} is the net specific rate of cell biomass, h^{-1}; μ_G is the specific growth rate of biomass, h^{-1}; k_d is the specific death rate of biomass, h^{-1}.

LA production processes traditionally suffer from end-product inhibition which limits not only microbial metabolism but also product formation (Axelsson, 1993). Although the pH of the fermentation broth in this study was maintained at 6.0 by automatic addition of 5M NaOH. The inhibition mechanism of LA is probably related to the solubility of the undissociated LA within the cytoplasmic membrane and the insolubility of dissociated lactate, which causes acidification of cytoplasm and failure of proton motive forces. It eventually influences the transmembrane pH gradient and decreases the amount of energy available for cell growth (Gonçalves, Ramos, Almeida, Xavier, & Carrondo, 1997). Therefore, the effects of end product inhibition must be taken into account in the kinetic modeling, as well as substrate limitation and growth conditions. As a result, for extracellular product formation, the Monod equation (Monod, 1949) is modified to show the end product inhibition:

$$\mu_P = \frac{r_P}{X} = \frac{\mu_{Pmax} S}{(K_{PS} + S)(1 + \frac{P}{K_P})} \tag{4.5}$$

where μ_P is the specific formation rate of product, h^{-1}; μ_{Pmax} is the maximum produuction formation rate, h^{-1}; K_{PS} is the saturation constant, g/L; K_P is the product inhibition constant, g/L.

Similarly, the Monod equation of cell biomass growth is modified as:

$$\mu_S = \frac{\mu_{max} S}{K_S + S} \frac{1}{1 + \frac{P}{K_P}} \tag{4.6}$$

where μ_S is the specific growth rate of cell biomass on substrate; μ_{max} is the maximum growth rate of cell biomass, h^{-1}; K_S is the saturation constant, g/L.

During batch growth, there are limiting nutrients for the cells to utilize and cell growth stops when running out of either carbon source or nitrogen source (Koller, 2018). In this study, the fermentation broth contained an abundant amount of carbon source, which was glucose, but a limited amount of nitrogen source. Therefore, cell concentration reached its maximum packing density when the limiting nitrogen source was completely utilized. As a result, the effect of limiting nitrogen source can be added to Eq. (4.6) as:

$$\mu_G = \frac{\mu_{max} S}{K_S + S} \frac{1}{1 + \frac{P}{K_P}} \frac{N}{K_N + N} \tag{4.7}$$

$$\mu_N = \frac{r_N}{X} = -\frac{\mu_{Nmax} S}{K_S + S} \frac{1}{1 + \frac{P}{K_P}} \frac{N}{K_N + N} \tag{4.8}$$

where N is the nitrogen concentration, g/L; K_N is the saturation constant, g/L; μ_N is the specific consumption rate of nitrogen source, h^{-1}; μ_{Pmax} is the maximum nitrogen source consumption rate, h^{-1}.

During the batch fermentation process in this study, the limiting substrate consumption is directly related to the cell biomass growth and product formation:

$$r_S = -\frac{\mu_S X}{\gamma F_{X/S}} - \frac{\mu_P X}{\gamma F_{P/S}} \tag{4.9}$$

where $\gamma F_{X/S}$ is the cell biomass growth yield factor, g/g; $\gamma F_{P/S}$ is the product

formation yield factor, g/g.

Since the volume is nearly constant during the batch fermentation, Eq. (4.1), (4.2), and (4.3) can be rearranged to give:

$$\frac{dX}{dt} = r_X = (\frac{\mu_{max}S}{K_S + S} \frac{1}{1 + \frac{P}{K_P}} \frac{N}{K_N + N} - k_d)X \tag{4.10}$$

$$\frac{dP}{dt} = r_P = \frac{\mu_{Pmax}S}{(K_{PS} + S)(1 + \frac{P}{K_P})} X \tag{4.11}$$

$$\frac{dS}{dt} = r_S = -\frac{\mu_{max}S}{K_S + S} \frac{1}{1 + \frac{P}{K_P}} \frac{X}{\gamma F_{X/S}} - \frac{\mu_{Pmax}S}{(K_{PS} + S)(1 + \frac{P}{K_P})} \frac{X}{\gamma F_{P/S}} \tag{4.12}$$

$$\frac{dN}{dt} = r_N = -\frac{\mu_{Nmax}S}{K_S + S} \frac{1}{1 + \frac{P}{K_P}} \frac{N}{K_N + N} X \tag{4.13}$$

4.2.2 Estimation of kinetic parameters

The Monod equation of cell growth is only applicable for balanced growth, at which pseudosteady state inside the cells has been reached (Galban & Locke, 1999). Thus, it is not applicable in the lag phase. To determine when to use the Monod equation, a straight line (dashed line) was drawn on the biomass growth curves as shown in Fig 4.13. It was observed that there was an apparent lag time t_L = 2 h and the cell concentration changed with time and became exponential after t= 3 h. Therefore, the data was correlated starting from t= 3 h.

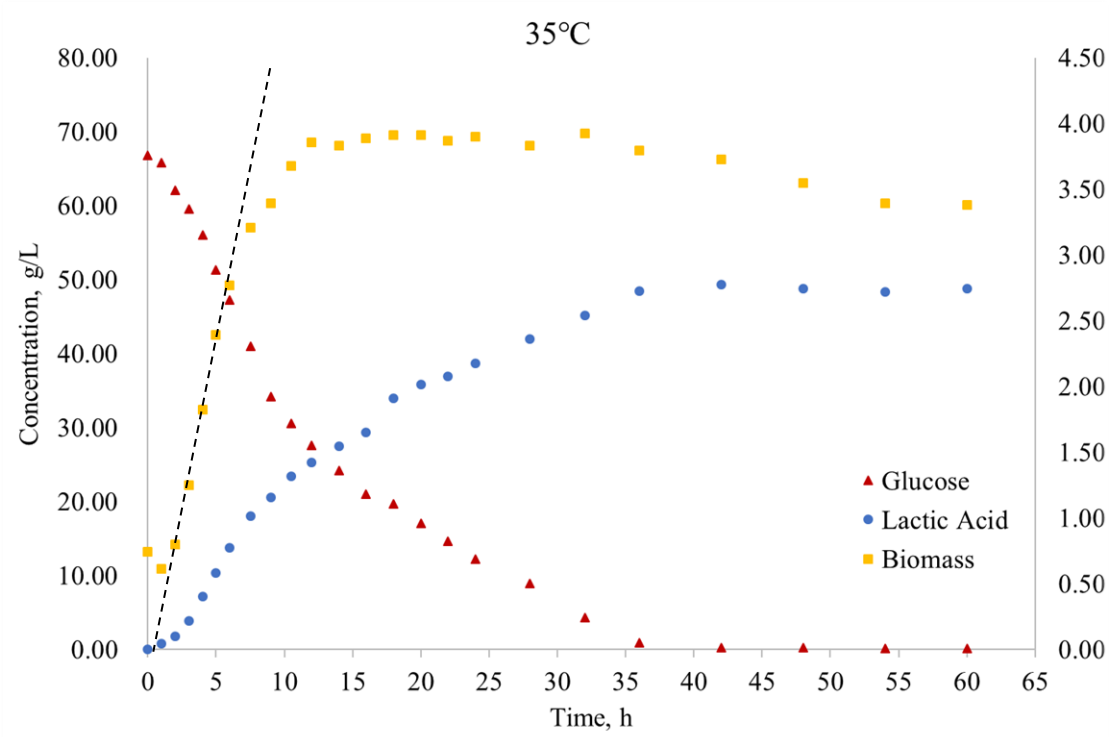

Figure 4.13 Profiles of glucose utilization, biomass growth and LA production during batch fermentation from glucose by *L. pentosus* at 35 ℃ and pH 6.0 (agitation speed at 150 rpm, and air flow rate at 25 mL/min). A dashed line was drawn as a guide on the cell biomass data.

Using the OdexLims in Excel to solve the four differential equations (Appendix K), while fitting with the experimental data, the kinetic parameters were obtained as: μ_{max} =12.266 h^{-1}, μ_{Pmax} =9.2077 h^{-1}, μ_{Nmax} =3.1730 h^{-1}, k_d =0.0062904 h^{-1}, K_S=166.97 g/L, K_{PS}=0.015488 g/L, K_P=0.17865 g/L, K_N=0.40135 g/L, $\gamma F_{X/S}$= 0.17865 g/g, $\gamma F_{P/S}$=0.98360 g/g. With all the kinetic parameters known, the growth behavior of the cells in the batch fermentation culture could be calculated or predicted.

For organisms growing aerobically on glucose, the cell biomass growth yield factor $\gamma F_{X/S}$ is typically 0.4-0.6g/g for most yeast and bacteria (Liu, 2016). As mentioned above, $\gamma F_{X/S}$ was estimated to be 0.1862 g/g, quite a lot lower than 0.4 g/g, which indicated that the limiting nitrogen source contained in the fermentation broth had successfully lowered cell growth, and accordingly left a larger portion of carbon source

for product formation.

4.2.3 Experimental data fitting

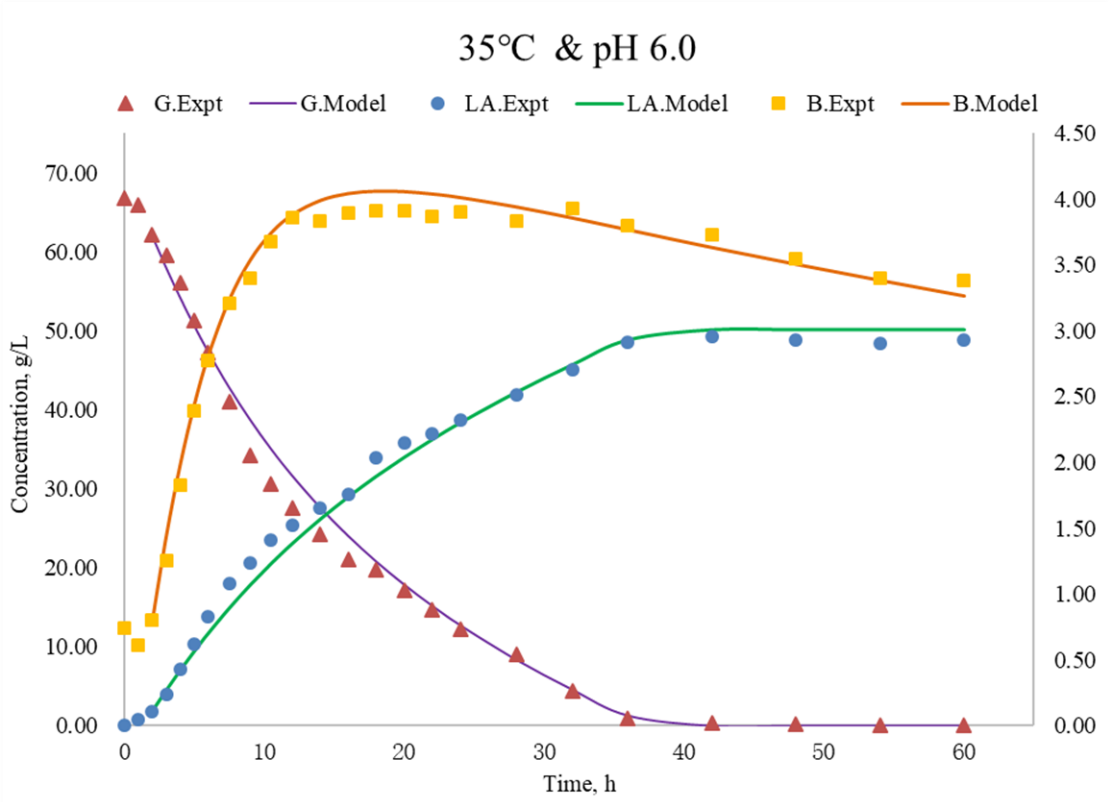

	G	B	LA
R^2	0.9835	0.9906	0.9932

Figure 4.14 Curve fitting of the predicted data to experimental data for glucose utilization, biomass growth and LA production for batch fermentation from glucose by *L. pentosus* at 35°C and pH 6.0 (agitation speed at 150 rpm, and air flow rate at 25 mL/min).

Expt: experiment data; Model: predicted data; G: glucose; B, biomass; LA, lactic acid.

From Fig 4.14, it could be observed that the developed model presented good agreement on cell growth, glucose utilization and LA production with the experimental results. The closeness between predicted and experimental data was further demonstrated by computing the squared Pearson correlation coefficient (Appendix L),

R^2 (0.9835-0.9932), which indicated that the developed model was able to predict the experimental results with high accuracy.

CHAPTER 5: CONCLUSION AND RECOMMENDATION

5.1 Conclusion

In this study, temperature effects during batch and continuous LA production were investigated. The main findings of this research included: (1) temperature effects on glucose utilization, cell growth and LA production by *L. pentosus* from glucose via batch fermentation process and (2) development of an unstructured kinetic model to describe batch LA production from glucose.

5.1.1 LA batch fermentation by *L. pentosus* from glucose

LA production by *L. pentosus* from glucose only follows EMP pathway because of the absence of measurable acetic acid and ethanol production. Rapid glucose utilization and LA production happen in the first 35 hours, and biomass growth tend to be steady after 12 hours.

5.1.2 Temperature effects on LA batch fermentation by *L. pentosus* from glucose

In batch fermentation of pH 6.0, agitation speed at 150 rpm and air flow rate at 25 mL/min, lower temperature leads to better cell growth while higher temperature results in more efficient glucose utilization and more productive LA generation. As temperature increases from 20 ℃ to 35 ℃, glucose is utilized faster and more fully, contributing to a shorter lag phase in cell growth and producing more LA with a higher productivity and a higher product yield. However, when temperature increases from 35 ℃ to 45 ℃, glucose utilization slows down and more glucose remains unconsumed,

extending the cell growth lag phase and generating less LA with lower productivities and product yields. In addition, the obtained biomass concentration and the fermentation time required to reach steady state decrease with temperature from 20 ℃ to 45 ℃.

5.1.3 Optimal temperature of LA batch fermentation by *L. pentosus* from glucose

The optimal temperature documented is 35 ℃ when pH is 6.0 during batch fermentation by *L. pentosus* from glucose (agitation speed at 150 rpm, and air flow rate at 25 mL/min).

5.1.4 Unstructured kinetic modeling of LA batch fermentation by *L. pentosus* from glucose

An unstructured kinetic model was developed to describe batch LA production at 35 ℃ and pH 6.0 from glucose by *L. pentosus*, when cell growth, glucose utilization, LA production, end product inhibition and limiting nitrogen source for cell growth were taken into account.

Kinetic parameters were determined by using Visual Basic Application (VBA) routine ODEXLIMS to solve a set of ordinary differential equations:

$$\frac{dX}{dt} = r_X = (\frac{\mu_{max} S}{K_S + S} \frac{1}{1 + \frac{P}{K_P}} \frac{N}{K_N + N} - k_d)X$$

$$\frac{dP}{dt} = r_P = \frac{\mu_{Pmax} S}{(K_{PS} + S)(1 + \frac{P}{K_P})} X$$

$$\frac{dS}{dt} = r_S = -\frac{\mu_{max} S}{K_S + S} \frac{1}{1 + \frac{P}{K_P}} \frac{X}{\gamma F_{X/S}} - \frac{\mu_{Pmax} S}{(K_{PS} + S)(1 + \frac{P}{K_P})} \frac{X}{\gamma F_{P/S}}$$

$$\frac{dN}{dt} = r_N = -\frac{\mu_{Nmax} S}{K_S + S} \frac{1}{1 + \frac{P}{K_P}} \frac{N}{K_N + N} X$$

and Excel solver to minimize the variance between experimental and predicted values. Kinetic parameters were estimated as: the maximum biomass growth rate μ_{max} =12.266 h^{-1}, the maximum product formation rate μ_{Pmax} =9.2077 h^{-1}, the maximum nitrogen source utilization rate μ_{Nmax}=3.1730 h^{-1}, the specific cell death rate k_d =0.0062904 h^{-1}, the saturation constants K_S =166.97 g/L K_{PS} =0.015488 g/L K_P=1.0928 g/L K_N=0.40135 g/L, the cell biomass growth yield factor $\gamma F_{X/S}$= 0.17865 g/g, the product formation yield factor $\gamma F_{P/S}$=0.98360 g/g.

The developed model was excellent in predicting biomass growth, product formation and substrate utilization with the squared Pearson correlation coefficients (R^2) of 0.9835, 0.9906 and 0.9932, respectively.

5.2 Recommendations for future work

5.2.1 Continuous fermentation

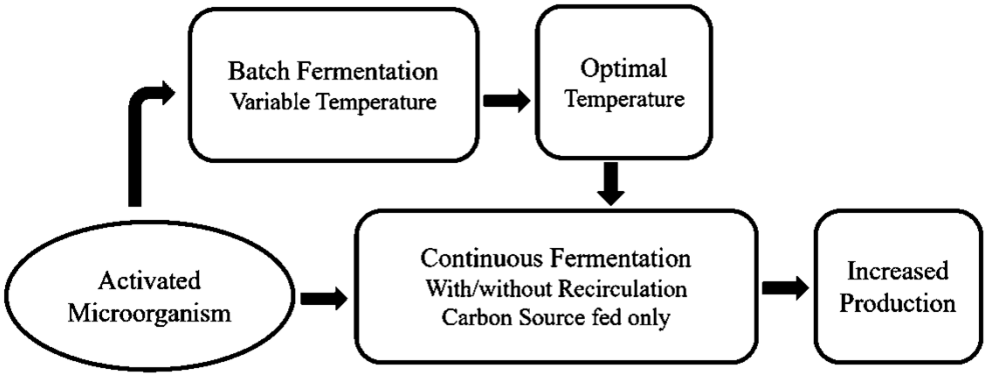

Figure 5.1 Experimental flow chart of continuous fermentation.

The temperature effects found in this study could be usefully tested in a continuous

fermentation process, based on results from the batch fermentation at 30 ℃, the optimal temperature for cell growth obtained in this study and then moving forward to apply in continuous fermentation at 35 ℃, the optimal temperature for glucose utilization and LA production obtained in this batch study. The batch data implies that best continuous results are likely to be found in the temperatures between 30 and 35 ℃. Used to take best advantage of the batch data, glucose is the only nutrient fed and cell recirculation.

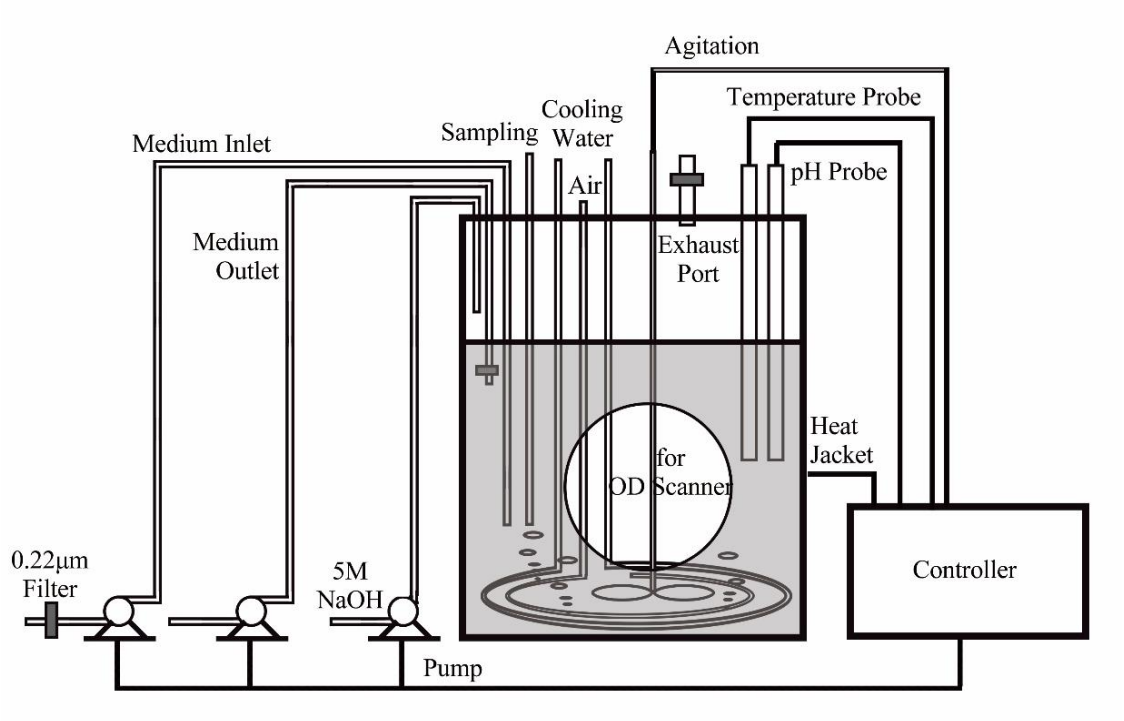

Figure 5.2 Schematic diagram of continuous fermentation system for reference.

5.2.2 Kinetic model improvement

The developed unstructured LA kinetic model could further be improved by including the effects of temperature and pH on kinetic parameters. It is also recommended to develop a structured model for batch LA production from glucose and compare the obtained kinetic parameters to the unstructured ones.

5.2.3 Additional screening of fermentation conditions by Plackett- Burman design

To further improve LA production via fermentation processes, it would be necessary to study the rest of the parameters affecting the fermentation process, such as carbon source, nitrogen source, especially pH effects on glucose utilization, biomass growth and LA production.

Table 5.1 Assigned parameters of variables at different levels in Plackett-Burman design for LA production by batch fermentation.

	Variables	Lower Level (-)	Higher Level (+)
1	X_1 Temperature	30 ℃	40 ℃
2	X_2 pH	6	7.5
3	X_3 Carbon Source	60 g/L Glucose	30 g/L Glucose+ 30 g/L Xylose
4	X_4 Nitrogen Source	10 g/L Yeast Extract	5 g/L Yeast Extract + 5 g/L Peptone
5	X_5 Inoculum Size	2 mL	5 mL
6	X_6 Working Volume	500 mL	800 mL
7	X_7 Air	Arobic	25 mL/min

Table 5.2 Plackett-Burman design for 7 variables with coded values.

Run	X_1	X_2	X_3	X_4	X_5	X_6	X_7
1	+	+	+	+	+	+	+
2	+	+	-	-	-	-	+
3	+	-	+	+	-	-	-
4	+	-	-	-	+	+	-
5	-	+	+	-	+	-	-
6	-	+	-	+	-	+	-
7	-	-	+	-	-	+	+
8	-	-	-	+	+	-	+

LITERATURE CITED

Abdel-Rahman, M. A., Tashiro, Y., & Sonomoto, K. (2013). Recent advances in lactic acid production by microbial fermentation processes. Biotechnology advances, 31(6), 877-902.

Agarwal, M., Koelling, K. W., & Chalmers, J. J. (1998). Characterization of the degradation of polylactic acid polymer in a solid substrate environment. Biotechnology progress, 14(3), 517-526.

Åkerberg, C., Hofvendahl, K., Zacchi, G., & Hahn-Hägerdal, B. (1998). Modelling the influence of pH, temperature, glucose and lactic acid concentrations on the kinetics of lactic acid production by Lactococcus lactis ssp. lactis ATCC 19435 in whole-wheat flour. Applied microbiology and biotechnology, 49(6), 682-690.

Akpa, J. (2012). Modeling of a bioreactor for the fermentation of palmwine by Saccaharomyce cerevisiae (yeast) and lactobacillus (bacteria). American Journal of Scientific and Industrial Research, 3(4), 231-240.

Alsaheb, R. A. A., Aladdin, A., Othman, N. Z., Malek, R. A., Leng, O. M., Aziz, R., & Enshasy, H. A. E. (2015). Lactic acid applications in pharmaceutical and cosmeceutical industries. J. Chem. Pharm. Res, 7, 729-735.

Axelsson, L. T. (1993). Lactic Acid Bacteria: Classification and Physiology,(dalam Lactic Acid Bacteria, S. Salminen and Ryanbakti Pranata Kusuma Teguh, 2014. Resting Suspensions of Lactobacillus delbrueckii,(dalam Lactic Acid Bacteria, S. Salminen and AV Wright, Eds), New York.

Axelsson, L., & Ahrné, S. (2000). Lactic acid bacteria. In Applied microbial systematics (pp. 367-388). Springer, Dordrecht.

Bieler, P. S. (2004). Analysis and modelling of the energy consumption of chemical batch plants. ETH Zurich.

Bouguettoucha, A., Balannec, B., & Amrane, A. (2011). Unstructured models for lactic acid fermentation–a review. Food Technology and Biotechnology, 49(1), 3-12.

Bustos, G., Moldes, A. B., Cruz, J. M., & Domínguez, J. M. (2005). Influence of the metabolism pathway on lactic acid production from hemicellulosic trimming vine shoots hydrolyzates using Lactobacillus pentosus. Biotechnology Progress, 21(3), 793-798.

Buyondo, J. P., & Liu, S. (2011). Lactic acid production by Lactobacillus pentosus from wood extract hydrolysates. J-FOR-Journal of Science and Technology for Forest Products and Processes, 1(3), 38.

Datta, R., & Henry, M. (2006). Lactic acid: recent advances in products, processes and technologies—a review. Journal of Chemical Technology & Biotechnology: International Research in Process, Environmental & Clean Technology, 81(7), 1119-1129.

De Vuyst, L., & Leroy, F. (2007). Bacteriocins from lactic acid bacteria: production, purification, and food applications. Journal of molecular microbiology and biotechnology, 13(4), 194-199.

Dusselier, M., Van Wouwe, P., Dewaele, A., Makshina, E., & Sels, B. F. (2013). Lactic acid as a platform chemical in the biobased economy: the role of chemocatalysis.

Energy & Environmental Science, 6(5), 1415-1442.

Fogler, H. S. (2010). Essentials of chemical reaction engineering. Pearson Education.

Fogler, H. S., & Brown, L. F. (1992). Distributions of residence times for chemical reactors. Elements of chemical reaction engineering, 708, 758.

Foutch, G. L., & Johannes, A. H. (2017). Reactors In Process Engineering. Oklahoma State University.

Galban, C. J., & Locke, B. R. (1999). Analysis of cell growth kinetics and substrate diffusion in a polymer scaffold. Biotechnology and Bioengineering, 65(2), 121-132.

Garde, A., Jonsson, G., Schmidt, A. S., & Ahring, B. K. (2002). Lactic acid production from wheat straw hemicellulose hydrolysate by Lactobacillus pentosus and Lactobacillus brevis. Bioresource Technology, 81(3), 217-223.

Gonçalves, L. M. D., Ramos, A., Almeida, J. S., Xavier, A. M. R. B., & Carrondo, M. J. T. (1997). Elucidation of the mechanism of lactic acid growth inhibition and production in batch cultures of Lactobacillus rhamnosus. Applied Microbiology and Biotechnology, 48(3), 346-350.

Griffiths, M. J., Garcin, C., van Hille, R. P., & Harrison, S. T. (2011). Interference by pigment in the estimation of microalgal biomass concentration by optical density. Journal of microbiological methods, 85(2), 119-123.

Hofvendahl, K. (1998). Fermentation of wheat starch hydrolysate by Lactococcus lactis: factors affecting product formation.

Hofvendahl, K., & Hahn–Hägerdal, B. (2000). Factors affecting the fermentative

lactic acid production from renewable resources1. Enzyme and microbial technology, 26(2-4), 87-107.

Holzgrabe, U. (2010). Quantitative NMR spectroscopy in pharmaceutical applications. Progress in Nuclear Magnetic Resonance Spectroscopy, 57(2), 229-240.

Hujanen, M., & Linko, Y. Y. (1996). Effect of temperature and various nitrogen sources on L (+)-lactic acid production by Lactobacillus casei. Applied microbiology and biotechnology, 45(3), 307-313.

Jin, T., & Zhang, H. (2008). Biodegradable polylactic acid polymer with nisin for use in antimicrobial food packaging. Journal of Food Science, 73(3), M127-M134.

Juliastuti, S. R., Baeyens, J., Creemers, C., Bixio, D., & Lodewyckx, E. (2003). The inhibitory effects of heavy metals and organic compounds on the net maximum specific growth rate of the autotrophic biomass in activated sludge. Journal of hazardous materials, 100(1-3), 271-283.

Krishna, R. H. (2013). Review of Research on Bio Reactors used in Wastewater Treatment for production of Bio Hydrogen: Future Fuel. International Journal of Science Inventions Today, 2(4), 302-310.

Koller, M. (2018). A review on established and emerging fermentation schemes for microbial production of Polyhydroxyalkanoate (PHA) biopolyesters. Fermentation, 4(2), 30.

Komesu, A., de Oliveira, J. A. R., da Silva Martins, L. H., Maciel, M. R. W., & Maciel Filho, R. (2017). Lactic acid production to purification: a review. BioResources, 12(2), 4364-4383.

Lee Rodgers, J., & Nicewander, W. A. (1988). Thirteen ways to look at the correlation coefficient. The American Statistician, 42(1), 59-66.

Leroy, F., & De Vuyst, L. (2004). Lactic acid bacteria as functional starter cultures for the food fermentation industry. Trends in Food Science & Technology, 15(2), 67-78.

Li, Y., & Cui, F. (2010). Microbial lactic acid production from renewable resources. In Sustainable biotechnology (pp. 211-228). Springer, Dordrecht.

Liu, S. (2016). Bioprocess engineering: kinetics, sustainability, and reactor design. Elsevier.

Lunt, J. (1998). Large-scale production, properties and commercial applications of polylactic acid polymers. Polymer degradation and stability, 59(1-3), 145-152.

Maier, R. M., & Pepper, I. L. (2015). Bacterial growth. In Environmental Microbiology (Third Edition) (pp. 37-56).

Martinez, F. A. C., Balciunas, E. M., Salgado, J. M., González, J. M. D., Converti, A., & de Souza Oliveira, R. P. (2013). Lactic acid properties, applications and production: a review. Trends in food science & technology, 30(1), 70-83.

Mason, C. A., & Egli, T. (1993). Dynamics of microbial growth in the decelerating and stationary phase of batch culture. In Starvation in bacteria (pp. 81-102). Springer, Boston, MA.

Myers, J. A., Curtis, B. S., & Curtis, W. R. (2013). Improving accuracy of cell and chromophore concentration measurements using optical density. BMC biophysics, 6(1), 4.

Monod, J. (1949). The growth of bacterial cultures. Annual Reviews in Microbiology, 3(1), 371-394.

Motta, S., & Pappalardo, F. (2012). Mathematical modeling of biological systems. Briefings in Bioinformatics, 14(4), 411-422.

Narayanan, N., Roychoudhury, P. K., & Srivastava, A. (2004). L (+) lactic acid fermentation and its product polymerization. Electronic journal of Biotechnology, 7(2), 167-178.

Newton, J. M. (2018). Understanding cell lysis in fermentation and its impact on primary recovery using viscosity monitoring (Doctoral dissertation, UCL (University College London)).

Nord, L. I., Vaag, P., & Duus, J. Ø. (2004). Quantification of organic and amino acids in beer by 1H NMR spectroscopy. Analytical chemistry, 76(16), 4790-4798.

Rai, R. K., & Chandel, V. S. (2015). Quantitative Metabolic Profiling of Human Serum by Nonlinear Sampling and Forward Maximum Entropy Reconstruction of Two-dimensional ^{1}H - ^{13}C HSQC. Journal of Physical Science, 26(1), 13.

Rogers, P. L., Bramall, L., & McDonald, I. J. (1978). Kinetic analysis of batch and continuous culture of Streptococcus cremoris HP. Canadian journal of microbiology, 24(4), 372-380.

Rolfe, M. D., Rice, C. J., Lucchini, S., Pin, C., Thompson, A., Cameron, A. D., ... & Peck, M. W. (2012). Lag phase is a distinct growth phase that prepares bacteria for exponential growth and involves transient metal accumulation. Journal of bacteriology, 194(3), 686-701.

Stevenson, K., McVey, A. F., Clark, I. B., Swain, P. S., & Pilizota, T. (2016). General calibration of microbial growth in microplate readers. Scientific reports, 6, 38828.

Taylor, J. (1997). Introduction to error analysis, the study of uncertainties in physical measurements.

Thongchul, N. (2013). Production of lactic acid and polylactic acid for industrial applications. Bioprocessing technologies in biorefinery for sustainable production of fuels, chemicals, and polymers, 293-316.

Todorov, S. D., & Dicks, L. M. T. (2004). Effect of medium components on bacteriocin production by Lactobacillus pentosus ST151BR, a strain isolated from beer produced by the fermentation of maize, barley and soy flour. World Journal of Microbiology and Biotechnology, 20(6), 643-650.

Towler, G., & Sinnott, R. K. (2012). Chemical engineering design: principles, practice and economics of plant and process design. Elsevier.

Vijayakumar, J., Aravindan, R., & Viruthagiri, T. (2008). Recent trends in the production, purification and application of lactic acid. Chemical and biochemical engineering quarterly, 22(2), 245-264.

Vu, T. H. T., Au, H. T., Nguyen, T. H. T., Nguyen, T. T. T., Do, M. H., Bui, N. Q., & Essayem, N. (2013). Esterification of lactic acid by catalytic extractive reaction: an efficient way to produce a biosolvent composition. Catalysis letters, 143(9), 950-956.

Wang, Y., Tashiro, Y., & Sonomoto, K. (2015). Fermentative production of lactic acid from renewable materials: recent achievements, prospects, and limits. Journal of

bioscience and bioengineering, 119(1), 10-18.

Wee, Y. J., Kim, J. N., & Ryu, H. W. (2006). Biotechnological production of lactic acid and its recent applications. Food Technology and Biotechnology, 44(2), 163-172.

Yumoto, I., & Ikeda, K. (1995). Direct fermentation of starch to L-(+)-lactic acid using Lactobacillus amylophilus. Biotechnology letters, 17(5), 543-546.

Yang, H. J., Yim, N. H., Lee, K. J., Gu, M. J., Lee, B., Hwang, Y. H., & Ma, J. Y. (2016). Simultaneous determination of nine bioactive compounds in Yijin-tang via high-performance liquid chromatography and liquid chromatography-electrospray ionization-mass spectrometry. Integrative medicine research, 5(2), 140-150.

Yumoto, I., & Ikeda, K. (1995). Direct fermentation of starch to L-(+)-lactic acid using Lactobacillus amylophilus. Biotechnology letters, 17(5), 543-546.

Zhang, J., Shao, X., Townsend, O. V., & Lynd, L. R. (2009). Simultaneous saccharification and co-fermentation of paper sludge to ethanol by Saccharomyces cerevisiae RWB222—Part I: Kinetic modeling and parameters. Biotechnology and bioengineering, 104(5), 920-931.

Zwietering, M. H., Jongenburger, I., Rombouts, F. M., & Van't Riet, K. (1990). Modeling of the bacterial growth curve. Applied and environmental microbiology, 56(6), 1875-1881.

APPENDICES

Appendix A: Standard curves for NMR spectroscopy and OD scanner.

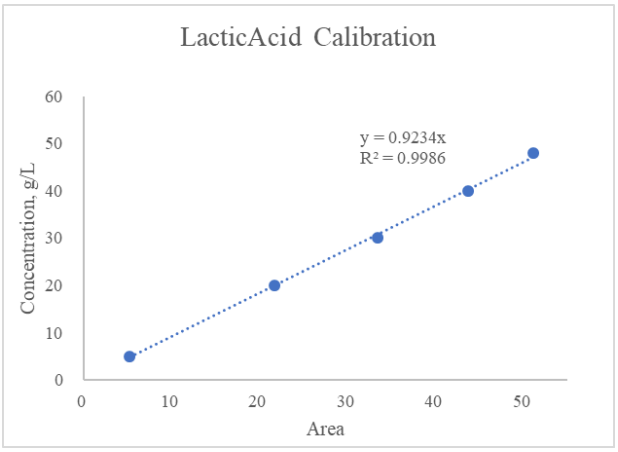

(a) lactic acid concentration versus integrated area from NMR spectrum

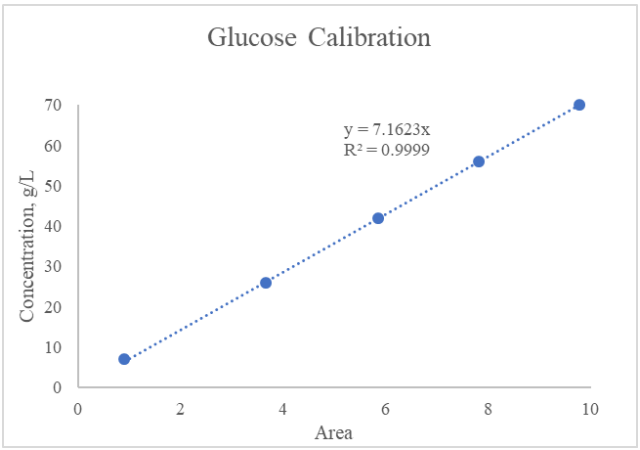

(b) glucose concentration versus integrated area from NMR spectrum

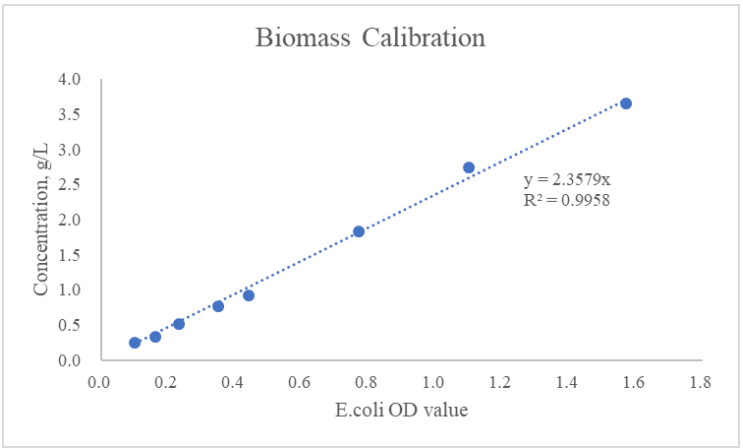

(c) *L. pentosus* biomass concentration versus *E.coli* OD value from OD scaner

Appendix B: Profiles of glucose utilization, biomass growth and LA production during batch fermentation at different temperatures (pH 6.0, agitation speed at 150 rpm, and air flow rate at 25 mL/min).

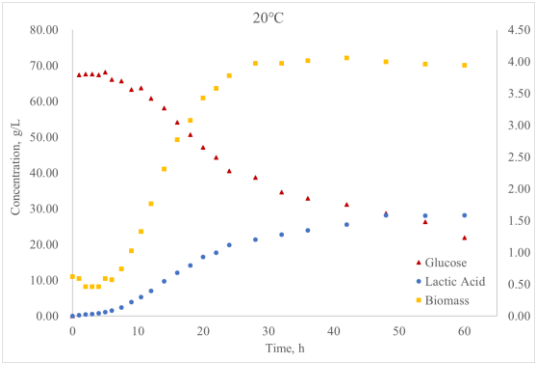

(a) profile of batch fermentation at 20 °C

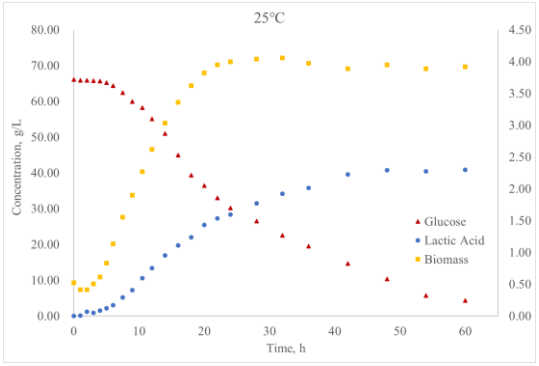

(b) profile of batch fermentation at 25 °C

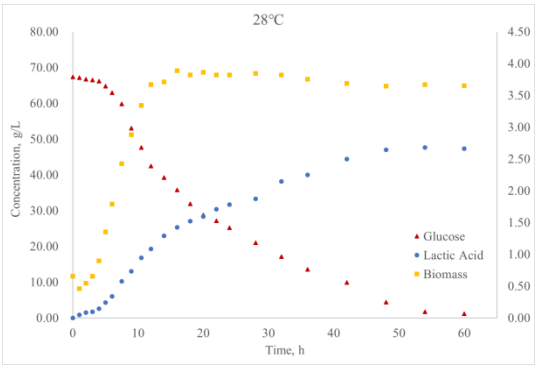

(c) profile of batch fermentation at 28 °C

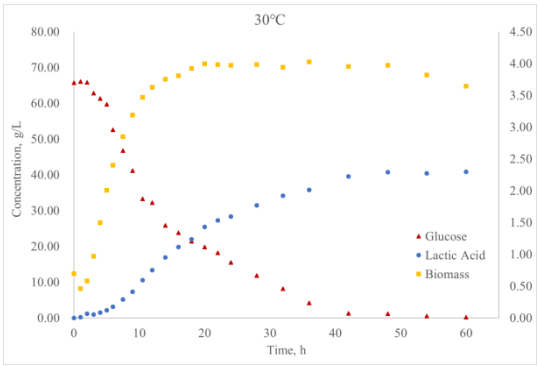

(d) profile of batch fermentation at 30 °C

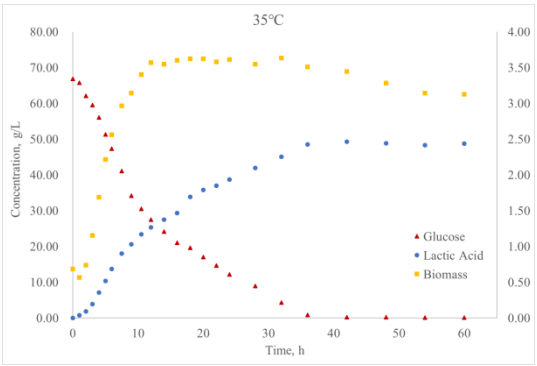

(e) profile of batch fermentation at 35 °C

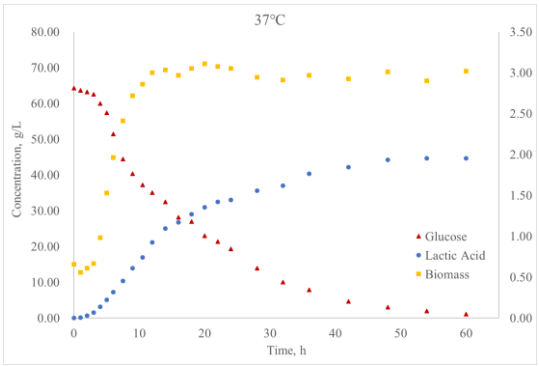

(f) profile of batch fermentation at 37 °C

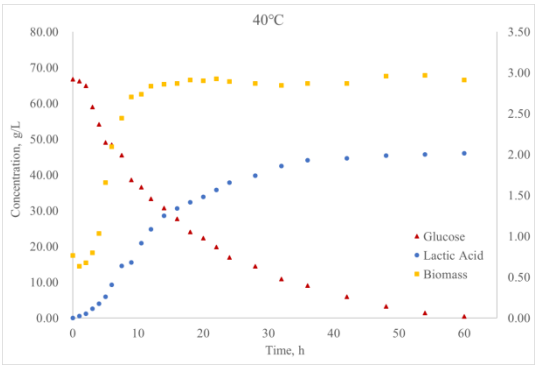

(g) profile of batch fermentation at 40 °C

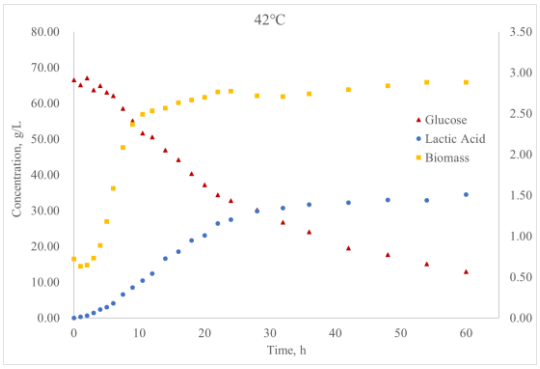

(h) profile of batch fermentation at 42 °C

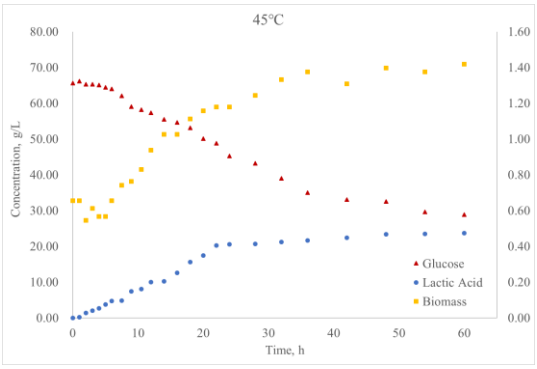

(i) profile of batch fermentation at 45 °C

Appendix C: Profiles of glucose utilization, biomass growth and LA production during batch fermentation at different pH (35 °C, agitation speed at 150 rpm, and air flow rate at 25 mL/min).

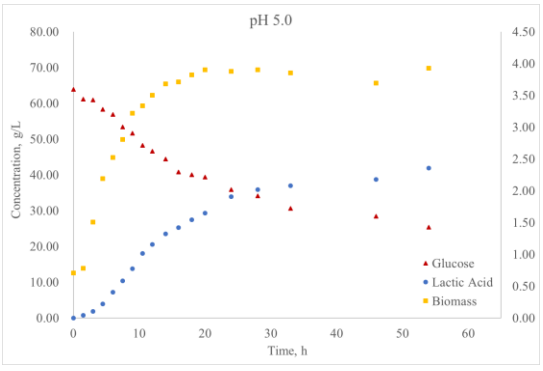

(a) profile of batch fermentation at pH 5.0

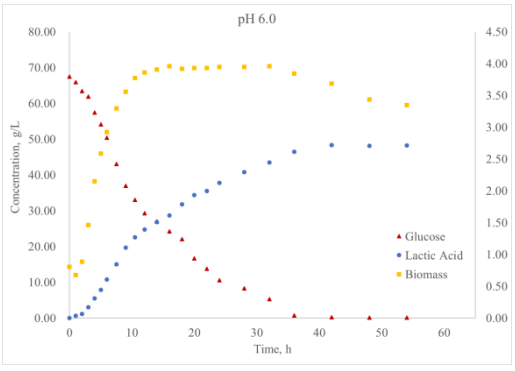

(b) profile of batch fermentation at pH 6.0

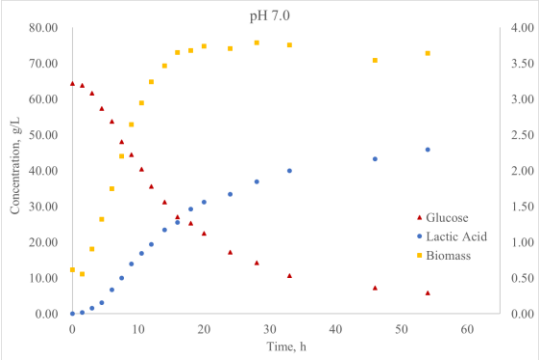

(c) profile of batch fermentation at pH 7.0

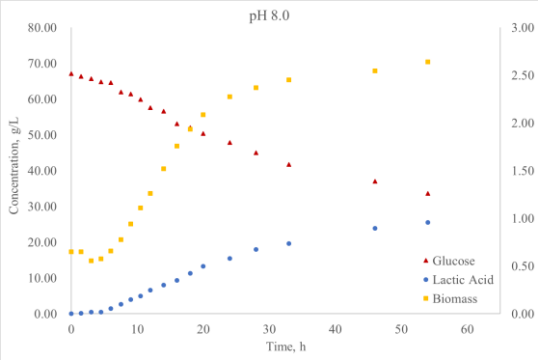

(d) profile of batch fermentation at pH 8.0

Appendix D: Influence of temperature on the glucose utilization during batch fermentation (pH 6.0, agitation speed at 150 rpm, and air flow rate at 25 mL/min).

T (°C)	20	25	28	30	35	37	40	42	45
G (%)	32.09	6.51	1.70	0.35	0.17	1.69	0.75	19.48	44.00
$\mu_{SE,max}$ (h^{-1})	1.71	2.40	3.85	3.93	4.24	4.02	3.74	2.05	1.62

T: temperature, degrees Celsius; G: residual glucose concentration, percentage of initial glucose concentration; $\mu_{SE,max}$: maximum glucose consumption rate obtained from experiment, per hour.

Appendix E: Influence of temperature on the biomass growth during batch fermentation (pH 6.0, agitation speed at 150 rpm, and air flow rate at 25 mL/min).

T (°C)	20	25	28	30	35	37	40	42	45
B (g/L)	3.94	3.92	3.65	3.64	3.13	3.02	2.91	2.88	1.42
$\mu_{GE,max}$ (g/(L•h))	0.26	0.26	0.39	0.45	0.49	0.47	0.47	0.37	0.06
t_L (h)	7.5	4	3	2	2	3	3	4	5
t_S (h)	28	22	16	16	14	12	12	12	32

T: temperature, degrees Celsius; B: biomass concentration, gram per liter; $\mu_{GE,max}$ maximum biomass growth rate obtained from experiment, per hour; t_L, time period of lag phase, hour; t_S, time required to reach stationary phase, hour.

Appendix F: Influence of temperature on the LA production during batch fermentation (pH 6.0, agitation speed at 150 rpm, and air flow rate at 25 mL/min).

T (℃)	20	25	28	30	35	37	40	42	45
LA (g/L)	28.09	40.86	47.30	48.05	48.75	44.66	46.01	34.50	23.69
$\mu_{PE,max}$ (h^{-1})	1.13	1.81	2.20	2.75	3.15	2.41	2.61	1.44	1.35
t_S (h)	48	48	48	42	36	36	32	28	22

T: temperature, degrees Celsius; LA: lactic acid concentration, gram per liter; $\mu_{PE,max}$: maximum LA formation rate obtained from experiment, per hour; t_S, time required to reach steady state, hour.

Appendix G: Influence of pH on the biomass growth, LA production and glucose utilization during batch fermentation (35 ℃, agitation speed at 150 rpm, and air flow rate at 25 mL/min).

pH	B g/L	LA g/L	G %	$Y_{P/S}$ g/g	Q_V g/(g•L•h)
5	3.93	25.37	39.67	0.6588	0.53
6	3.96	48.27	0.13	0.7158	1.01
7	3.79	45.93	9.04	0.7842	0.96
8	2.64	25.58	50.12	0.7639	0.53

B: biomass concentration, gram per liter; LA: lactic acid concentration, gram per liter;

G: residual glucose concentration, percentage of initial glucose concentration; $Y_{P/S}$: product yield, gram LA per gram consumed glucose; Q_V: volumetric LA productivity, gram LA per gram consumed glucose per liter per hour.

Appendix I: Influence of temperature on the biomass growth, LA production and glucose utilization during batch fermentation (pH 6.0, agitation speed at 150 rpm, and air flow rate at 25 mL/min).

T	B g/L	LA g/L	G %	$Y_{P/S}$ g/g	Q_V g/(g•L•h)
20℃	4.39	28.09	32.09	0.6138	0.59
25 ℃	4.39	40.86	6.51	0.6618	0.85
28 ℃	4.20	47.30	1.70	0.7139	0.99
30 ℃	4.29	48.05	0.35	0.7332	1.00
35 ℃	3.93	48.75	0.17	0.7308	1.02
37 ℃	3.36	44.66	1.69	0.7072	0.93
40 ℃	3.21	46.01	0.75	0.6945	0.96
42 ℃	3.11	34.50	19.48	0.6448	0.72
45 ℃	1.53	23.69	44.00	0.6446	0.49

T: temperature, degrees Celsius; B: biomass concentration, gram per liter; LA: lactic acid concentration, gram per liter; G: residual glucose concentration, percentage of initial glucose concentration; $Y_{P/S}$: product yield, gram LA per gram consumed glucose; Q_V: volumetric LA productivity, gram LA per gram consumed glucose per liter per hour.

Appendix J: Relative error is a measure of the uncertainty of measurement compared to the size of the measurement (Taylor, 1997). The relative error is defined by

$$\delta_x = \frac{\Delta x}{x} = \frac{x_0 - x}{x} = \frac{x_0}{x} - 1$$

where Δx is the absolute error, x_0 is the measured or inferred value, x is the true value. In this work, x is the experimental data obtained in the batches of the study of temperature effects and x_0 is the experimental data gathered verification experiment of pH effects.

Appendix K: Visual basic module showing the integral kernels and the excel work sheet for estimation of kinetic parameters in this study.

Let y(1) = X, y(2) = S, y(3) = P, y(4) =N,

c(1) =μ_{max}, c(2) =μ_{Pmax}, c(3) =μ_{Nmax}, c(4) =k_d,c(5) =K_S, c(6) =K_{PS}, c(7) =K_P,

c(8) =K_N, c(9) =$\gamma F_{X/S}$, c(10) =$\gamma F_{P/S}$,

and the independent variable $x = t$.

```
  Option Base 1
Option Explicit

'The following subroutine defines the ordinary differential equations   y'=f(x,y,c)
'You may change the lines within Sub Func and Sub Jacobian
'Report bugs to Dr. Shijie Liu

Sub Func(f, ByVal x As Double, ByVal y, Optional c)

f(1) = (c(1) * y(2) / (c(5) + y(2)) * y(4) / (c(8) + y(4)) / (1 + y(3) / c(7)) - c(4)) * y(1)
f(3) = c(2) * y(2) / (c(6) + y(2)) / (1 + y(3) / c(7)) * y(1)
f(2) = -c(3) * y(2) / (c(5) + y(2)) / (1 + y(3) / c(7)) * y(1) / c(9) - c(2) * y(2) / (c(6) + y(2)) / (1 + y(3) / c(7)) * y(1) / c(10)
f(4) = -c(3) * y(2) / (c(5) + y(2)) * y(4) / (c(8) + y(4)) / (1 + y(3) / c(7)) * y(1)


End Sub
```

T. h	Conc. g/L				μmax	μpmax	μnmax	kd	Ks	Kps	Kp	Kn	yFx/s	yFp/s
	X	S	P		12.266	9.2077	3.1730	0.0062904	166.97	0.015488	1.0928	0.40135	0.17865	0.98360
					X, cal	S, cal	P, cal	N, cal	error,X	error,S	error,P			
0	0.7427	66.8289	0.0000					-	-	-	-			
1	0.6131	65.8289	0.7869					-	-	-	-			
2	0.8017	62.1235	1.8530		0.8017	62.1235	1.8530	1.0000	0.0000	0.0000	0.0000			
3	1.2497	59.5760	3.8921		1.4473	58.0531	4.5182	0.8311	0.0391	2.3193	0.3921			
4	1.8274	56.0443	7.1580		1.99	54.2570	7.0452	0.6879	0.0265	0.0319	0.0001			
5	2.3933	51.3546	10.3309		2.4414	50.7165	9.4405	0.5676	0.0023	0.0041	0.0079			
6	2.7705	47.3018	13.7576		2.8111	47.4146	11.7101	0.4676	0.0016	0.0001	0.0419			
7.5	3.2067	41.0490	18.0642		3.2362	42.8732	14.8920	0.3503	0.0009	0.0333	0.1006			
9	3.3954	34.1592	20.6025		3.5362	38.7765	17.8272	0.2644	0.0198	0.2132	0.0770			
10.5	3.6783	30.5696	23.4708		3.7415	35.0710	20.5398	0.2024	0.0040	0.2026	0.0859			
12	3.8552	27.5590	25.3153		3.8778	31.7066	23.0539	0.1578	0.0005	0.1720	0.0511			
14	3.8316	24.2009	27.4983		3.9856	27.6743	26.1370	0.1171	0.0237	0.1206	0.0185			
16	3.8905	21.0745	29.3174		4.0382	24.0773	28.9569	0.0904	0.0218	0.0902	0.0013			
18	3.9141	19.6850	33.9286		4.0563	20.8419	31.5547	0.0726	0.0202	0.0134	0.0564			
20	3.9141	17.0796	35.8408		4.0526	17.9091	33.9640	0.0603	0.0192	0.0069	0.0352			
22	3.8670	14.6479	36.9915		4.0348	15.2323	36.2116	0.0518	0.0282	0.0034	0.0061			
24	3.9023	12.2163	38.7006		4.0077	12.7747	38.3193	0.0457	0.0111	0.0031	0.0015			
28	3.8316	8.9740	41.9496		3.9367	8.4035	42.1820	0.0382	0.0110	0.0033	0.0005			
32	3.9259	4.3423	45.1225		3.8531	4.6192	45.6569	0.0345	0.0053	0.0008	0.0029			
36	3.7962	0.9264	48.4900		3.7629	1.3075	48.8099	0.0330	0.0011	0.0015	0.0010			
42	3.7255	0.2895	49.3192		3.6288	0.0001	50.0863	0.0329	0.0094	0.0008	0.0059			
48	3.5486	0.2316	48.8284		3.5019	(0.0000)	50.0863	0.0329	0.0022	0.0005	0.0158			
54	3.3954	0.1158	48.3292		3.3801	0.0000	50.0863	0.0329	0.0002	0.0001	0.0309			
60	3.3823	0.1158	48.7523		3.2618	0.0000	50.0863	0.0329	0.0145	0.0001	0.0178	error,SUM		
									0.2627	3.2213	0.9505	4.4345		

Appendix L: In statistics, the Pearson correlation coefficient is a measure of the linear correlation between two variables X and Y. It has a value between +1 and −1, where 1 is total positive linear correlation, 0 is no linear correlation, and −1 is total negative linear correlation. Pearson correlation coefficient is the covariance of the two variables divided by the product of their standard deviations (Lee & Nicewander, 1988). Given a pair of random variables (X, Y), the formula for Pearson correlation coefficient ρ is:

$$\rho_{X,Y} = \frac{\mathrm{cov}\,(X,Y)}{\sigma_X \sigma_Y}$$

Where cov is the covariance, σ_X is the standard deviation of X, σ_Y is the standard deviation of Y.

In this work, X is the experimental data and Y is the predicted data. $\rho_{X,Y}$ is used to show the closeness of the experimental and predicted date for glucose utilization, LA production and biomass growth.